Russian Chemical Reviews **72** (7) 571 – 589 (2003) © 2003 Russian Academy of Sciences and Turpion Ltd

DOI 10.1070/RC2003v072n07ABEH000799

Low-temperature reactions in the chemistry of nanosystems

T I Shabatina, G B Sergeev

Contents

I.	Introduction	571
II.	General peculiarities of low-temperature chemical reactions	571
III.	Reactions of metal atoms and small clusters in low-temperature matrices	574
IV.	Reactions in quantum crystals and superfluid helium nanodroplets at ultralow temperatures	576
V.	Reactions in low-temperature film co-condensates	577
VI.	Cryochemical synthesis and reactions involving metal nanoparticles	578
VII.	Assembly of hybrid nanostructures at low temperatures	579
VIII.	Conclusion	585

Abstract. The results of recent investigations on the reactions proceeding at low and ultra-low temperatures are considered. Trends in development of new avenues of cryochemical research, related to reactions of metal atoms, clusters and nanoparticles and to processes occurring in quantum nanocrystals and superfluid helium nanodroplets are analysed. Specific features of the formation of films and metal-containing nanosystems at low temperatures are discussed. The bibliography includes 265 references.

I. Introduction

Most chemical compounds at low (10 – 100 K) and ultralow (0.2 – 10 K) temperatures are in the solid state. Under such conditions, the diffusional mobility is restricted. According to the Arrhenius equation, the rates of chemical processes decrease as temperature decreases, so the reactions become nearly 'frozen' at temperatures close to 100 K. These general considerations underlie the development of efficient methods for cryoconservation of various chemical, food and biological products. Nevertheless, the midtwentieth century was marked by the discovery of unusual fast (nearly explosive) reactions proceeding at low and ultralow temperatures. These are reactions of free radicals, halogens and halocarbons with unsaturated compounds, polymerisation of reactive monomers and some other processes.[1–4]

Advances made in cryochemistry during the last decade include the development of methods for generation and stabilisation of metal atoms and small clusters, metastable complexes and nanoparticles, the number of metal atoms in which varies from several to hundreds and thousands.[5–8] These high-energy and highly reactive species can participate in various low-temperature chemical reactions resulting in novel hybrid materials possessing unusual optical and electronic properties and in highly active sensor and catalytic systems. Cryocondensates with encapsulated metal nanoparticles can be considered as novel chemical energy sources and storage systems.

Of particular interest are low-temperature size effects due to dependence of the reactivity of metal clusters and nanoparticles on the number of constituent atoms. Indeed, such systems provide examples of development of a new research avenue, *viz*., cryonanochemistry. The dependences of diffusion parameters, mechanical stabilities and reactivities of samples of organic and organometallic condensates and co-condensates on the thickness of the growing films can also be considered as the effects specific to cryochemistry. Thus, in cryochemical studies it is possible to draw a line between the microscopic and macroscopic properties of systems comprising atoms, clusters and nanoscale particles.

In this review we analyse experimental data on unusual low-temperature reactions and new phenomena accompanying these processes. We present some examples of chemical reactions in supersonic jets, quantum crystals and liquid helium droplets and on the surfaces of ice crystallites and cosmic dust particles in the interstellar medium. Considerable attention is given to self-assembly of inorganic clusters and nanoparticles in structured polymer matrices and ordered mesogenic systems, resulting in the formation of anisotropic metal – polymer and metal – mesogenic nanosystems. We also illustrate the possibility of targeted preparation of nanostructured materials with prescribed properties.

II. General peculiarities of low-temperature chemical reactions

Radicals, molecules and metal atoms and clusters are usually stabilised using different variants of the low-temperature matrix isolation technique and preparative cryochemistry, which are also employed to study chemical reactions of these species. Usually, low-temperature chemical reactions proceed under conditions of layer-by-layer or co-condensation of reactant vapours or an inert matrix on continuously cooling surfaces of various cryostats *in vacuo*. It should be noted that reactions at the gas – solid, gas – liquid and solid – solid interfaces are also possible. Often, carrying out a chemical reaction between two substances in a co-condensate film requires preliminary formation of labile complexes of the reactants to provide an optimum orientation of the species in the course of mutual diffusion. Evolution of the surface structure and energetics of chemical reactions are studied by structural methods, microscopy, thin-film calorimetry and spectroscopy.

T I Shabatina, G B Sergeev Department of Chemistry, M V Lomonosov Moscow State University, Leninskie Gory, 119992 Moscow, Russian Federation. Fax (7-095) 939 02 83. Tel. (7-095) 939 54 42.
E-mail: tsh@kinet.chem.msu.ru (T I Shabatina), gbs@kinet.chem.msu.ru (G B Sergeev)

Received 5 March 2003
Uspekhi Khimii **72** (7) 643 – 663 (2003); translated by A M Raevsky

1. Sample preparation on cold surfaces: specific features

Sample preparation techniques are critical to cryochemical research. Currently, two methods are most widely used. The first of them, the matrix isolation method, involves co-condensation of the compound under study with a large excess (from a hundred to a thousand times) of inert component (usually, an inert gas or hydrocarbon).[9,10]

This technique allowed the discovery and investigation of a new class of compounds, *viz*., metastable complexes of photochemically generated Rg_n-HX and $H-Rg-X$ (Rg = He, Xe, Ar; X is electron-acceptor group, *e.g*., OH, SH or F, Cl, I) molecules. These species are stabilised in low-temperature matrices of inert gases.[11,12] Quantum-chemical calculations of their electronic structures were reported.[13,14] Chaban *et al*.[14] studied xenon insertion into some organic molecules (*e.g*., $HXeC_2H$, $HXeC_6H_5$, $HXeOC_6H_5$) and predicted the existence of stable inclusion compounds and linear oligomers $H(XeC_2)_nXeH$ ($n \geqslant 1$). The matrix isolation technique has been successfully used for stabilisation and spectroscopic studies of radical and molecular intermediates in pyrolysis and photolysis reactions.[15] It permits identification of labile complexes, various isomers and conformers and investigations of their interconversions.[16] A method for stabilisation and spectroscopic investigation of radicals and short-lived intermediates on an activated silica gel surface has been proposed.[17,18]

The second approach is based on co-condensation of reactant vapours on cooled surfaces at rates that exclude collisions between the reactant molecules in the gas phase (molecular beam condensation).[19] Possible modifications of this technique include, *e.g*., condensation of particles of the same type; layer-by-layer condensation of particles of different types; co-condensation of particles of different types; co-condensation of reactive species with a large excess of inert component; co-condensation of reactive species with a third component (an activator or initiator). In all cases the system can be additionally activated by irradiating samples,[20,21] exposing them to high-frequency, ultrasonic and heat fields [22,23] and by mechanochemically treating them.[24,25] For instance, reactions of photogenerated mobile fluorine atoms with the O_3, NH_3, C_2H_4 and HCN molecules in argon matrices at 10–40 K have been studied in detail by EPR, IR and optical spectroscopies.[26]

A general scheme of physicochemical processes occurring during condensation of atoms and molecules on cooling surfaces is presented in Fig. 1. Condensation-driven growth of a film sample can be accompanied by accommodation effects, surface diffusion, tunnelling interaction, clustering and nucleation. These processes are determined by such parameters as the condensation rate (particle flux through a unit of surface area per unit time) and the surface temperature. Raising the temperature causes diffusion of small particles, which were produced and stabilised in the first stage, in the matrix followed by formation of larger particles and clusters. Clearly, processes occurring (i) in the course of interaction between atom and molecular beams and the surface and (ii) on subsequent heating of the samples are of crucial importance. They determine specific features of low-temperature chemical reactions and control the morphology of newly formed surface nanostructures.

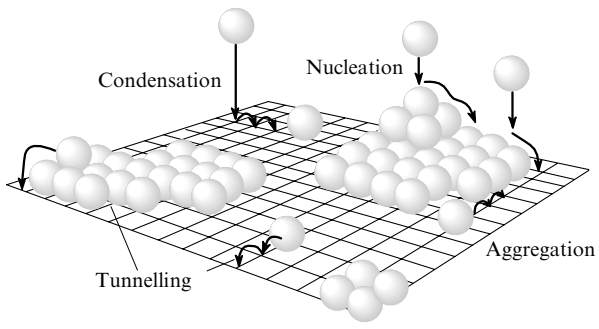


Figure 1. A scheme of physicochemical processes occurring during condensation of atoms and molecules on a cold surface.

The most stubborn problem is to predict and describe those properties of low-temperature film co-condensates that are due to their inhomogeneity and nonequilibrium nature. There are two important consequences. First, reactive species in low-temperature co-condensates are kinetically and thermodynamically nonequivalent. Second, particles stabilised at low temperatures possess an excess energy (as compared to the mean energy of particles at a given temperature) and, as a rule, high reactivity upon addition of a third reactive component. Therefore, low-temperature co-condensates can be considered as chemical energy storage systems. The excess energy stored in the growing film of a low-temperature co-condensate can be estimated taking into account the following data: the excess energies of metastable crystalline and amorphous phases range from 5 to 20 kJ mol^{-1}, the energies of donor–acceptor interactions and complexation lie between 10 and 40 kJ mol^{-1}, the enthalpies of exothermic chemical reactions are 100 to 200 kJ mol^{-1}, the excess energies of stabilised reactive species (atoms and small clusters) or the recombination energies of radicals vary from 100 to 400 kJ mol^{-1} and the energy of mechanical stress is nearly 10 kJ mol^{-1} (see Ref. 7).

2. Size effects

The size effects manifest themselves as dependences of the physical and chemical properties of particles under study on the number of constituent atoms. Usually, they are divided into two main groups. These are internal size effects associated with nonmonotonic change in the bulk-to-surface atom ratio and external size effects due to the interaction of particles of different sizes and shapes with external electric and magnetic fields. The former group of effects is due to changes in the structural and electronic characteristics of particles including their reactivity, binding energy, ionisation potential, melting point, crystal structure parameters, *etc*.[27–36] External size effects manifest themselves as co-operative electron or lattice excitations, which in the case of, *e.g*., metal nanoparticles are responsible for the appearance of electron–plasmon resonance bands in the optical spectra.[37–39]

Two types of size effect can be distinguished in cryochemistry. One of them is the effect of the size of the reacting species (number of structural units, *i.e*., atoms or molecules) on the mechanism and kinetics of their chemical transformations.[40] The other effect is the influence of the thickness of the growing low-temperature co-condensate film on its reactivity.[41,42] In both cases small variations of the size parameters cause changes in the chemical properties of the system. Studies of interrelations between the reactivity and size of the reacting species (thickness of condensate films) are a topical avenue of cryochemical research.

High reactivity of metal nanoparticles is due to the presence of uncompensated chemical bonds of the surface atoms. According to calculations, almost all of the 10 to 15 atoms constituting a 1-nm particle can be considered as the surface atoms, while 10-nm particles ($\sim 10^4-10^6$ atoms) have only 15% of the atoms on the surface. The size effect is illustrated in Fig. 2 in which we present data on the reactivities of niobium clusters of different sizes, prepared using supersonic jet and mass selection techniques, in reactions with alkyl bromides.[43]

The particle size can be considered as a thermodynamic property determining the state and reactivity of the system at low temperatures. In Fig. 3, the relative reactivities of metal particles are schematically shown as functions of their sizes. According to this scheme, the reactivity reduces as follows: free atoms > oligomeric clusters > nanoparticles > aggregates > bulk metal. Thus, metal atoms and small clusters are the most reactive species. Usually, their properties are investigated using the matrix isolation technique at liquid helium temperatures. An

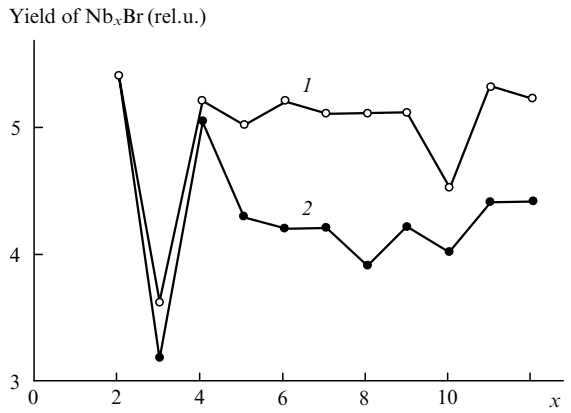


Figure 2. Cluster-size dependences of reactivities of niobium clusters Nb_x in reactions with EtBr (*1*) and Pr^iBr (*2*);[43] x is the number of atoms in the cluster.

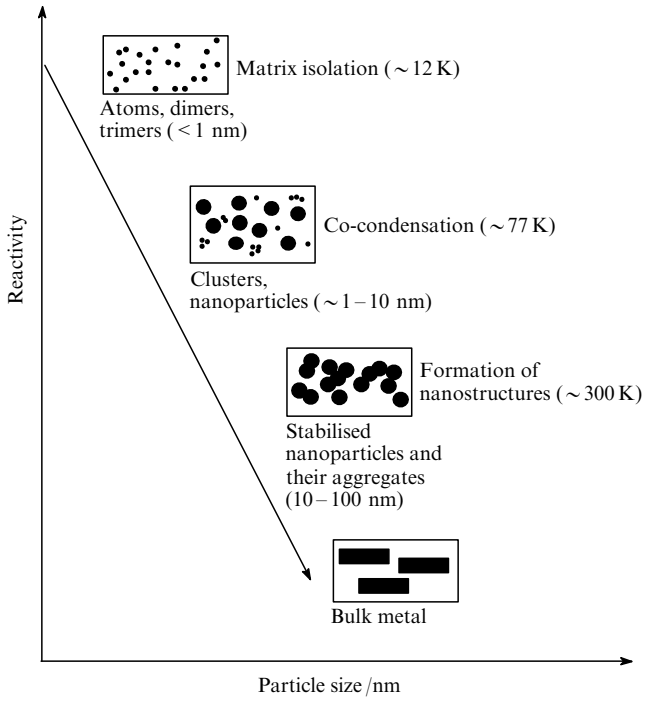


Figure 3. A scheme illustrating changes in the relative reactivities of metal particles as functions of their sizes and temperature of the reaction system.

increase in the particle size reduces the reactivity. It should be noted that this dependence is nonmonotonic because more stable particles, *e.g.*, the so-called magic clusters, are periodically formed. The reactivity is reduced to the greatest extent upon aggregation of small clusters, *i.e.*, as the properties of the aggregates become more and more similar to those of bulk material.

The particle size and reactivity can be preset using some experimentally controllable parameters, *e.g.*, the substrate temperature, metal-to-ligand (inert component) ratio, reactant condensation rate, heat treatment regime of samples and the presence of activators or stabilisers. As the condensation temperature decreases and the proportion of the inert component increases, diffusion-controlled processes in the system become less intense. Using this correlation, it is possible to stabilise high-energy and highly reactive particles in low-temperature matrices. The ratio of the reactant condensation rates usually has a strong effect on the size of the particles formed at a given temperature. As the metal-to-ligand ratio and temperature increase, the proportion of metal clusters and aggregated particles increases. The reactant condensation rates affect the properties of the growing condensate film in a complex manner. When highly reactive particles (atoms, dimers, trimers) are deposited on a cold surface, their lifetimes are inversely proportional to the condensation rate, being also dependent on the nature of relaxation processes in the system. The collision numbers of the reactant molecules with the surface and with one another are functions of the flux intensity of the particles being deposited. The above-mentioned factors and the chemical nature of the reactants govern the pathways and kinetics of low-temperature chemical reactions.

3. Defects and mechanical stress in the growing surface films

Various defects and mechanical stress produced during the growth of condensate films affect low-temperature chemical processes.[40,41] Analysis of elastic deformations responsible for initiation of chemical reactions in a film sample[40] showed that the formation of a co-condensate film begins with growth of islands. The growing islands can merge together, thus forming close-packed columnar aggregates. Interfacial interactions produce mechanical stress. As the growing film thickens, the columnar aggregates increase in size. After reaching a critical film thickness, cracking occurs, being accompanied by structural phase transitions that initiate fast chemical reactions and crystallisation. The initial amorphous system has an excess free energy. An increase in internal mechanical stress during condensation of reactants causes deformation and cracking of the film upon reaching a critical film thickness. Plastic deformations are responsible for enhancement of molecular mobility in the system and subsequent acceleration of chemical processes. Elastic deformations and cracks 'initiate' fast crystallisation of amorphous films.

Development of elastic deformation and occurrence of chemical reactions are interconnected by a feedback. This is a possible reason for autowave chemical transformations in the system during the growth of co-condensate film. The system's behaviour is determined by the particle size, the extent of deviation from the equilibrium state and by the rates of relaxation processes. This approach provides a qualitative explanation for the dependence of the reactivity of the film co-condensate on the growth conditions. Raising the temperature causes enhancement of the molecular mobility, thus favouring the growth of the existing nuclei rather than nucleation. The process is accompanied by relaxation of internal stress due to a decrease in the interface area. This causes weakening of mechanical stress and thickening of the sample.

Mechanical stress and critical thickness of a growing film were measured in a study of condensation of a water film using a low-temperature tensometer and calorimeter.[42] The results obtained confirmed the existence of an interrelation between spontaneous crystallisation of the film and chemical transformations in the sample. Thus, low-temperature co-condensation is accompanied by generation and storage of the mechanical energy, development of elastic and plastic deformations in the sample, enhancement of the molecular mobility in the system and by cracking. These processes can initiate chemical reactions in the system.

Release of excess energy stored in the mechanically non-equilibrium matrix component of a frozen bulk sample *via* brittle fracture of the sample has been studied.[44] Initiation of autowave chemical transformations in irradiated, cryochemically stabilised samples subjected to local fracture was observed during chlorination of saturated hydrocarbons, hydrobromination of olefins and polymerisation of 2-methylbuta-1,3-diene. γ-Radiation energy storage in the course of low-temperature radiolysis of solid HCN results in accumulation of stabilised radicals in the matrix.[45]

III. Reactions of metal atoms and small clusters in low-temperature matrices

Metal atoms and small clusters are highly reactive species. Because of this, investigations on their spectral and chemical properties require the use of special equipment and the matrix isolation technique. In particular, the Al_3, Cu_3, Ag_3, Ga_3 and Au_2Ag clusters were studied by EPR spectroscopy[46] using isolation in matrices of inert gases and hydrocarbons. Dimers and higher clusters of various metals (Na_n, Ag_n, Au_n, Cr_n, Mn_n, Sc_n, Y_n, Ln_n; $n = 2-9$) were investigated by UV and photoelectron spectroscopies, a fluorescence technique and using quantum-chemical calculations.[47–51] Currently, matrix isolation of mass-selected clusters is employed to obtain and perform spectroscopic studies of clusters and fragment ions of prescribed size.[52–56] The matrix isolation method allowed one to synthesise, stabilise and spectroscopically investigate a large number of coordinatively saturated and unsaturated metal complexes with N_2, O_2, CO, CO_2, C_2H_4 and C_2H_2.[57–61]

Both UV and electron (ion) beam initiated elementary reactions in low-temperature matrices are accompanied by electronic and structural relaxation of the cryomatrices containing various 'host' atoms, molecules and ions.[62,63] Interactions between reactive species including recombination of atoms, radicals and ions are often accompanied by luminescence and exoelectron emission.[64] Using data on thermally and photo-assisted exoelectron emission and luminescence, one can obtain information on the mobility mechanisms of neutral and charged reactive species and on the electronic relaxation in metastable matrices containing various additives.[65,66] The mechanisms of diffusion and electron transport in atomic and molecular cryomatrices (N_2, CH_4, CD_4, Ar and Kr) have been discussed.[67–69]

As mentioned above, unusual chemical reactions occurring at low temperatures cannot be performed under normal conditions. A general problem of cryochemistry is the impossibility of predicting the chemical behaviour of low-temperature systems containing metal atoms, clusters and nanoparticles based on the properties of bulk samples. Detailed investigations on the conditions for and mechanisms of low-temperature reactions involving metal atoms and clusters have been reported.[5–8] When studying reactions of atoms and small clusters, a third reactive component is often introduced in the low-temperature matrix doped with the metal atoms or clusters to provide an additional thermal or photochemical activation of the system. The most impressive examples of such studies are given below.

Reactions of the first-row transition metals with CO_2 and its isoelectronic analogues (CS_2 and OCS) in argon matrices were studied by UV and Fourier IR spectroscopies and by density functional quantum-chemical calculations.[70–74] These reactions are of interest from the standpoint of activation of the CO_2 molecule to involve it in low-temperature catalytic transformations. The results obtained show that these transition metals (Fe, Co, Ni and Cu) form 1 : 1 complexes with CO_2, whereas atoms of the early elements (Sc, Ti, V, Cr) insert into C–O bonds to give oxocarbonyls. Two isomeric $Ni-CO_2$ complexes differing in stability were found in the carbon dioxide matrix at 10 K.[72] The yields of the complexes dramatically decrease upon dilution of the system with argon. When using a nitrogen matrix, complexation enhances, resulting in more stable complexes $Ni(CO_2)(N_2)$ and $Ni(CO_2)(N_2)_2$. A co-operative effect of two ligands was pointed out. Namely, coordination of the nitrogen molecule causes hybridisation of the 4s and 3d orbitals of the nickel atom, which increases the degree of $Ni \rightarrow CO_2$ charge transfer in the structure of the biligand complex compared to the monoligand complex $Ni(CO_2)$. An analogous effect was observed in a study of the reaction of copper vapours with dinitrogen.[74] Co-condensation of copper with dinitrogen taken in excess results in $Cu_2(N_2)$ and $Cu_2(N_2)_2$ complexes with ease. Dilution of the system with argon causes a dramatic decrease in the yields of the complexes, while introduction of CO enhances complexation and favours the formation of mixed biligand complexes.

Reactions of magnesium atoms and clusters with CO_2 and ethylene were studied in argon matrix at 10–80 K (the metal species were stabilised) and in low-temperature co-condensates at 77–100 K by IR and UV spectroscopies and by chromatography.[75–77] Both the experimental data and the results of quantum-chemical calculations of the reaction system indicate formation of four- and five-membered cyclic complexes in the first stage.[78] *Ab initio* MP2/6-31G(d) and QCISD/6-31G(d) calculations[79] showed that conversion of CO_2 into CO occurs much more easily in the presence of Mg atoms:

$$Mg + CO_2 \longrightarrow MgO + CO.$$

The reaction is spin allowed and the potential barrier to the $CO_2 \rightarrow CO$ conversion becomes nearly halved; however, the reaction is still highly endothermic. The reverse reaction

$$MgO + CO \longrightarrow Mg + CO_2$$

is an exothermic process with a potential barrier of 2.8 kcal mol^{-1}.

Reactions of samarium atoms and clusters with ethylene in the temperature range 12–30 K result in π-complexes $Sm(C_2H_4)$ and $Sm(C_2H_4)_2$.[80,81] An unexpected effect was observed in studies of reactions of metals (Mg and Sm) with a mixture of C_2H_4 and CO_2. Under identical conditions samarium reacts only with CO_2, whereas magnesium forms complexes with both ligands.[80] The results obtained demonstrate different reactivity of metal atoms and clusters.

Unusual behaviour of magnesium atoms and clusters in reactions with halocarbons has been reported.[82–85] In particular, carbon tetrachloride does not react with bulk magnesium at ambient temperatures. The situation changes in the case of co-condensation of magnesium vapour and CCl_4 at 77–80 K. Magnesium atoms and clusters efficiently react with CCl_4 to give a variety of intermediates and stable products.[75]

$$Mg + CCl_4 \longrightarrow \begin{cases} CCl_3MgCl \xrightarrow{H_2O} CHCl_3 \\ CCl_3^{\bullet} \longrightarrow C_2Cl_6 \\ CCl_2^{\bullet\bullet} \longrightarrow C_2Cl_4 \end{cases}$$

The spectra of $Mg/CCl_4/Ar$ (Mg : Ar = 1 : 1000) co-condensates at 12 K first of all exhibited a decrease in the intensity of absorption of small magnesium clusters followed by consumption of magnesium atoms (Fig. 4).[83] The results of IR spectroscopic study showed that the major reaction products are C_2Cl_6 and C_2Cl_4.

Magnesium atoms and clusters possess different reactivities in reactions with alkyl(aryl) halides (RX, X = F, Cl, Br, I).[84] Magnesium atoms initiate radical recombination and disproportionation reactions with the formation of various products. Reactions in Mg/RX co-condensates (Mg : RX = 1 : 1 to 1 : 100) resulted in aggregation of magnesium atoms and preferred formation of CCl_3MgCl (a Grignard reagent). Magnesium and calcium clusters were shown to be more reactive species than the corresponding atoms.[86] The relative reactivity of metal particles in reactions with alkyl halides reduces as follows: $Ca_2 > Mg_4 > Mg_3 > Mg_2 > Ca > Mg$. The reactivity of methyl halides reduces in the order $CH_3I > CH_3F > CH_3Br > CH_3Cl$.

Co-condensation of sodium, magnesium and samarium vapours with alcohols causes a competition between two processes, *e.g.*,[75]

$$Sm \longrightarrow \begin{cases} \xrightarrow[80\ K]{ROH} RSmOH \xrightarrow[80\ K]{ROH} RH + (RO)_{1.5}Sm(OH)_{1.5} \\ \xrightarrow{\text{aggregation}} Sm_n \xrightarrow[80-300\ K]{ROH} Sm(OR)_3 + H_2 \end{cases}$$

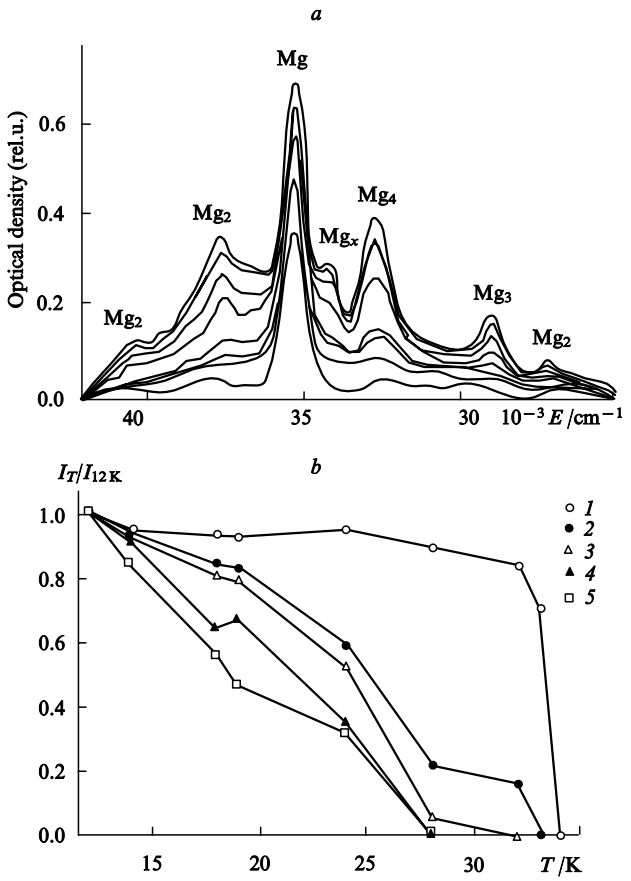


Figure 4. Absorption spectra of 1 : 100 : 1000 $Mg/CCl_4/Ar$ co-condensate (temperature increases from the top down in the range 12 to 34 K) (*a*) and temperature dependence of the normalised integrated intensity of absorption of magnesium atoms and clusters in this co-condensate (*b*).[83] Mg (*1*), Mg_4 (*2*), Mg_x (*3*), Mg_3 (*4*) and Mg_2 (*5*).

At 77 K, metal atoms stabilised at low metal concentrations (metal : ligand ≈ 1 : 500) reduce alcohols to hydrocarbons. Metal clusters formed in co-condensates at metal-to-ligand ratios of about 1 : 5 form alcoholates.[87]

The dependence of the reactivity of metal particles on the co-condensation conditions was confirmed by the results of studies on the synthesis and catalytic properties of samarium–hydrocarbon co-condensates[88] with hexane, cyclohexane, hex-1-ene and cyclohexene chosen as the model compounds. Comparison of the catalytic systems obtained by low-temperature co-condensation of (i) samarium and hexane and (ii) samarium and cyclohexene revealed higher activity of the former system in the hydrogenation of hex-1-ene. Similar results were obtained in studies of cyclohexene hydrogenation using a catalytic system prepared by low-temperature co-condensation of samarium and cyclohexane. Thus, there is a 'matrix memory' effect, *i.e.*, the system prepared by low-temperature co-condensation governs the reactivity and selectivity of subsequent catalytic transformations. It is possible to draw an analogy to enzymatic reactions, where the enzyme–substrate interactions are accompanied by rearrangement of the active site to match the substrate structure.

A systematic study of co-condensates of some transition metals with CH_4/Ar mixtures at 10 K was carried out by Klabunde *et al.*[89] Oxidative insertion of electronically excited metal atoms into C–H bonds has been reported.[90] The reactions of laser ablated iron atoms with methane and ethylene were studied by Mössbauer and IR spectroscopies in doped argon matrices at 17 K; quantum-chemical calculations of newly formed species and stable products were also performed.[89,90] The excited iron atoms are inserted into the C–H bond of methane to give CH_3FeH.[91] The first reaction stage involves decomposition of methane molecule to give a methyl radical $CH_3^{\bullet}$ and a hydrogen atom. The reaction in a methane matrix results in products of the interaction between primary radicals $CH_3^{\bullet}$ and H atoms with one another (C_2H_6, C_2H_4, C_2H_2) and with iron atoms, *viz.*, compounds CH_3FeH and $Fe_2H_2(CH_3)_4$ with Fe–H–Fe bridging bonds. Reactions of iron atoms with dilute ethylene in argon matrix give a $Fe(C_2H_4)$ complex. As the concentration of ethylene increases, complex $Fe(C_2H_4)_2$ becomes the major product. A study by Mössbauer spectroscopy revealed the formation of monomeric and dimeric halides FeF_3 and Fe_2F_6 and FeI_2 and Fe_2I_4 in the reactions of iron with halogen donors SF_6 and CH_3I.[92,93]

Co-condensation of transition metal atoms with aromatic hydrocarbons at 77–80 K often results in bisarene complexes of (formally) zero-valent metals.[94] For instance, co-condensation of lanthanide atoms and 1,3,5-tris-*tert*-butylbenzene produces thermally stable 'sandwich' complexes of Nd, Tb, Dy, Ho, Er and Lu, as well as thermally unstable complexes of La, Pr, Sm, Eu, Tm and Yb.[94] Metal complexes with phosphorus and nitrogen derivatives of aromatic hydrocarbons have been synthesised.[94] Reactions of titanium and vanadium vapours with 1,4-di-*tert*-butylbuta-1,3-diene resulted in novel compounds of general formula $[M(\eta^2\text{-}Bu^t_2C_4H_2)_2]$ (M = Ti, V).[95] The complexes obtained can be modified by introducing various ligands, *e.g.*, phosphines, diazadienes and isonitriles, which replace the diene ligand, thus forming novel 'half-sandwich' complexes.

Low-temperature co-condensates of lanthanides (Sm, Eu) with mesogenic ligands 4-pentyl-4′-cyanobiphenyl (5CB) and 4-octyl-4′-cyanobiphenyl (8CB) were studied by IR and UV spectroscopies in the temperature range 90–300 K. Formation of two labile complexes with 1 : 2 and 1 : 1 metal-to-ligand ratios was established.[96,97] Complex $Sm(CB)_2$ undergoes a solid-phase transformation into $Sm_2(CB)_2$ (CB is 4-alkyl-4′-cyanobiphenyl) in the temperature range 170–210 K. The process exhibits a polychronous kinetics,[97] which can be due to the presence of some solid-phase reactivity distribution of the complexes.[98] The IR spectra of Sm/5CB co-condensates with various metal-to-ligand ratios were studied at 95–273 K and at 95 K. Two new (compared to the IR spectrum of a neat 5CB film) bands with maxima at 2135 and 2085 cm^{-1} were observed in the region of stretching vibrations of the CN group. Based on a nearly 100 cm^{-1} shift towards the low-frequency region, these bands were assigned to the absorption bands of π-complexes. At 90–95 K, the spectrum of co-condensate exhibits a single absorption band at 2135 cm^{-1}. The absorption at 2085 cm^{-1} increases, while the absorption at 2135 cm^{-1} decreases on heating of the sample from 95 to 213 K. Thus, here we deal with conversion of one complex into the other. In addition, changes in the band intensity ratio upon variation of the metal-to-ligand ratio suggest the presence of two complexes of different compositions.[97] The UV and visible spectra of Sm/5CB film co-condensates revealed two new overlapped absorption bands with maxima at 390 and 420 nm.[97] Absorption in this spectral region is characteristic of charge-transfer complexes of transition metals with molecules of unsaturated organic compounds. The band intensities are also temperature dependent. This trend serves as an additional argument in favour of the existence of two complexes.

Labile 1 : 1 complexes of difluorostannylene (a hetero-element carbene analogue) with some aromatic molecules (benzene, chlorobenzene and toluene) were obtained and characterised by matrix IR spectroscopy.[99] Co-condensation of vanadium and chromium vapours with tetraphenylsilane ligands results in stable 'sandwich' complexes. Low-temperature co-condensation of vapours was employed to prepare novel di- and trinuclear clusters of molybdenum, rhenium and palladium.[100] Iron complexes containing η^6-arenes and trichlorosilyl ligands (Fig. 5) were also synthesised by co-condensation of vapours of the corresponding reactants.[101]

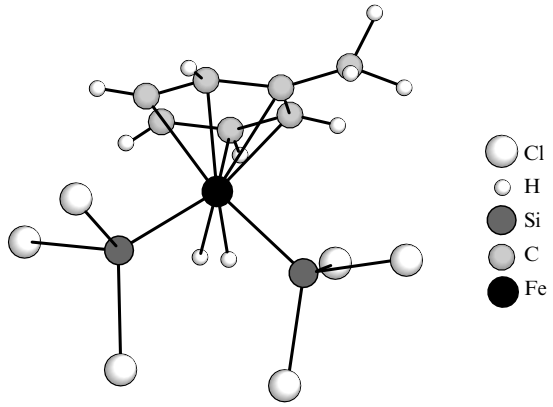


Figure 5. Structure of iron complexes containing η^6-arenes and trichlorosilyl ligands.[101]

Reaction products of iron atoms with polycyclic aromatic hydrocarbons (PAH) pyrene and coronene were studied by UV and Fourier IR spectroscopies in argon and nitrogen matrices.[102] The spectra of the co-condensates revealed the presence of mononuclear π-complexes of iron atom with pyrene, $Fe(C_{16}H_{10})_n$ (n = 1, 2), which are stable at temperatures of up to 24 K. In the structure of the π-complex, the iron atom is above the centre of one of the two outer aromatic rings. Formation of unstable Fe–H complexes with one or two hydrogen atoms of one aromatic ring of the ligand molecule or with two hydrogen atoms of different rings was also detected. The coronene molecule, which contains a large number of fused aromatic rings, preferentially reacts with iron dimer to give π-complexes $Fe_2(C_{24}H_{12})_n$ (n = 1, 2). These species are thermally stable up to the sublimation temperature of the argon matrix (40 K) and exhibit stability to 200–700 nm radiation. Two iron atoms can be arranged above two adjacent aromatic rings of the same ligand molecule or perpendicular to the ring plane, thus bonding two ligand molecules. The latter type of bonding can result in 'multi-sandwich' complexes. Relatively stable iron–PAH compounds comprising several iron atoms, small (nanoscale) iron aggregates formed under the action of external factors and thin films on carbon surfaces can be responsible for characteristic 3.3, 7.8, 8.6 and 11.3 μm IR radiation, which is often observed in space.[103–105]

IV. Reactions in quantum crystals and superfluid helium nanodroplets at ultralow temperatures

The use of quantum crystals (solid ^{3}He, ^{4}He, ortho- and para-hydrogen, HD)[106–109] and nanodroplets of quantum liquids (superfluid liquid helium) as matrices is of particular interest for investigations of chemical reactions at ultralow temperatures.[110–113]

Here, one deals with weak intermolecular interactions (absence of matrix effects), absence of 'cage effects' for photo-induced processes and quantisation of rotational motion of guest molecules. As a consequence, IR spectra exhibit narrow spectral lines with fully resolved rotational structure.[114–116] The effects observed are of great importance for astrophysics and astrochemistry[117,118] because the most abundant substances in space are hydrogen, helium and products of their ionisation by cosmic rays (H_2^+, H_3^+ and He^+).

The use of superfluid helium nanodroplets (He_N, $N \approx 10^2$–10^5) as matrices opens up new prospects for investigations of atoms, clusters, metastable molecules and complexes.[119] Nanodroplets are prepared by supersonic expansion of helium gas jets under high pressure at low temperatures. Surface evaporation causes cooling of a nanodroplet, so a temperature of 0.2 to 0.4 K is maintained inside it. Atoms and molecules can be included into helium nanodroplets by trapping the dopant in the gas phase

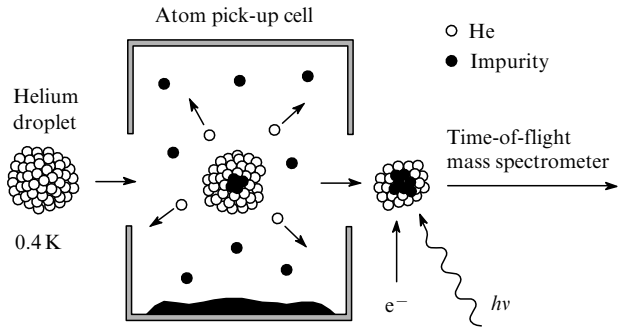


Figure 6. A scheme of formation of helium nanodroplets containing encapsulated impurity atoms (molecules).[120]

(Fig. 6).[120–123] Molecules, clusters and loosely bound complexes can be synthesised immediately during trapping of dopant atoms (molecules) into helium nanodroplets. Currently, this method is employed to obtain and perform spectral characterisation of alkali metal,[124,125] magnesium[120] and silver[126,127] clusters and rubidium–helium exciplexes.[128] Alkali metal atoms form loosely bound surface states due to Coulombic repulsion between the helium electrons and the valence electrons of the metal. The van der Waals metal clusters formed on the surface of nanodroplets are in the high-spin state. This phenomenon was studied by femtosecond multiphonon ionisation spectroscopy.[121] The mass distribution of spin-polarised clusters is shown in Fig. 7. Thus, even large clusters (N > 10) are completely spin-polarised. The observed alternation of the intensities of the peaks corresponding to clusters of different sizes is due to specific features of the mechanism of laser-induced spin relaxation.

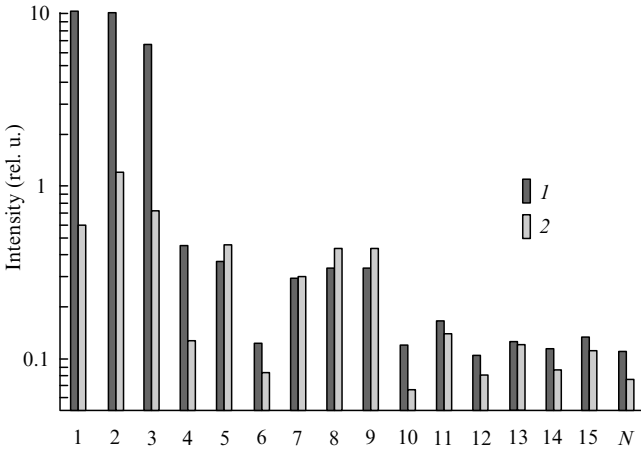


Figure 7. Mass distribution of Na_N clusters (N is the number of atoms in clusters). Laser excitation at 850 (*1*) and 425 nm (*2*).[121]

The vibronic spectra of mixed clusters M^4He_N and M^3He_N comprising aromatic molecules (M) and helium atoms have been studied at 0.4 K.[129] Taking these systems as examples, the intramolecular fine vibronic structure of $S_0 \rightarrow S_1$ electronic transitions in the spectra of various molecules was experimentally studied. Peculiar features of formation of atomic and molecular clusters during free gas expansion in vacuum have been considered.[130]

The structures of impurity systems prepared by trapping D_2, Ne, N_2 and Kr into the bulk of superfluid ^{4}He were studied by X-ray diffraction and ultrasonically.[131] The van de Waals interactions between the components result in the formation of a nanoscale system similar to aerogel, which comprises clusters of impurity molecules and atoms of size 50 ± 20 Å and density of up

to 10^{20} atom cm^{-3}. The possibility of stabilisation of high concentrations of atoms in such systems makes them promising energy sources. Water nanoclusters surrounded by layers of solid and liquid helium have been reported. They form a specific 'watergel', which acts as a matrix stabiliser and a dispersion medium.[131, 132]

Unusual tunnelling chemical reactions of light impurity atoms and molecules

$$D + H_2 \longrightarrow HD + H,$$

$$D + HD \longrightarrow D_2 + H$$

were investigated in solid helium at ~1.35 K.[133, 134] Deuterium atoms efficiently replace hydrogen atoms in the H_2 and HD molecules, thus favouring accumulation of rather high steady-state concentrations of hydrogen atoms (up to 10^{18} cm^{-3}).

An EPR study of tunnelling reactions of hydrogen atoms produced by γ-radiolysis of a mixture of ortho- and parahydrogen at 4.2 K [135, 136] showed that diffusion of atoms in solid hydrogen occurs by repeating tunnelling reactions

$$H + p\text{-}H_2 \longrightarrow p\text{-}H_2 + H$$

and is completed with a highly exothermic reaction

$$H + H(+M) \longrightarrow H_2(+M),$$

where M is a third particle acting as an energy drain.

Radiolysis of solid parahydrogen containing small amounts of deuterium impurity at 4.2 K causes formation of electron 'bubbles' that dissociate *via* tunnelling recombination with cations stabilised in the system.[137] In both cases the efficiency of tunnelling reactions is determined by weak interactions with orthohydrogen impurity and by energy dissipation in the matrix.[135] The contributions of two main mechanisms (sequential two-body process involving quasi-bound resonant states and tunnelling and a direct three-body recombination involving matrix atoms or molecules) to atom–atom recombination in matrices of inert gases have been analysed.[138, 139]

Studies on photoinduced reactions of dopant molecules (CH_4, CO_2, NO) in solid parahydrogen matrices have been reported.[140, 141] The absence of cage effects for the primary radicals and efficient reactions of 'hot' photofragments

$$CH_2 + H_2 \longrightarrow CH_4,$$

$$CO_2 + H \longrightarrow CO + OH,$$

$$OH + H_2 \longrightarrow H_2O + H,$$

$$NO + H \longrightarrow HNO,$$

$$N + 2H_2 \longrightarrow NH_3 + H,$$

$$O + H_2 \longrightarrow H_2O$$

are due to weak intermolecular interactions with the matrix molecules.

The possibility of using tunnelling reactions of hydrogen atoms for hydrogenation of various organic and inorganic compounds under conditions of cryochemical synthesis has been considered.[142, 143] Experiments carried out at 10 K showed that cyclic olefins (cyclopentene and cyclohexene) nearly instantaneously (in a few seconds) react with hydrogen atoms to give the corresponding cyclic alkanes.[142, 143] The reaction of hydrogen atoms with solid CO results in quantitative yields of formaldehyde and methanol.[144] The last-mentioned compound is efficiently formed upon additional UV irradiation of the system. These laboratory studies have first demonstrated the possibility of synthesis of these compounds in interstellar ice as a result of tunnelling reactions of hydrogen atoms with CO molecules. It was also shown that matrix-stabilised C, O and N atoms can be involved in reactions occurring on spraying H atoms over solid samples at 10 K. The reactions result in CH_4, H_2O and NH_3. The authors of this study [144] considered the possibility of tunnelling

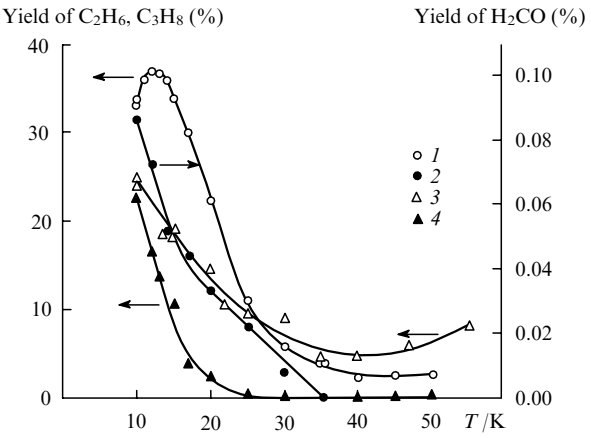


Figure 8. Yields of products of tunnelling reactions of H atoms with C_2H_4 (*1*), CO (*2*), C_3H_6 (*3*) and C_2H_2 (*4*) as functions of temperature in the range 10–60 K.[144]

interaction of H atoms with acetylene, ethylene, propylene and carbon monoxide in the temperature range 10–60 K. In all the cases the reaction rates increase as the temperature decreases from 50 down to 10 K and reach maximum values at 10 K (Fig. 8). Negative temperature dependence of the rate constant for tunnelling reaction of hydrogen atoms with acetylene in highly dilute samples in xenon or carbon dioxide matrices was unambiguously proved. The effect observed was explained by the possibility of increasing the steady-state concentration of hydrogen atoms in the solid film and by an increase in the rate constant for tunnelling reaction on lowering the temperature. Negative temperature dependences of the rate constants for tunnelling reactions were theoretically predicted by Hiraoka and Sato.[144] The influence of various factors (mutual arrangement of atoms, structural rearrangement of reactants and medium, orientational intermolecular vibrations) on the rates of tunnelling reactions and on the temperature dependence of the rate constants for tunnelling reactions involving hydrogen atoms has also been analysed.[139, 145–149]

V. Reactions in low-temperature film co-condensates

Vacuum co-condensation of reactant vapours on cooled surfaces of spectral and preparative cryostats provides conditions that exclude collisions between the reactant molecules in the gas phase. As a rule, in this case the reaction occurs within a thin surface layer. On heating, chemical reactions proceed in the bulk of the sample due to enhancement of the molecular mobilities of the reactants. In Fig. 9 we present a general scheme of successive and concerted reactions occurring in the course of low-temperature co-condensation of vaporous metals (M) and various organic or inorganic ligands (L). At low temperatures and high dilutions, reactions of metal atoms mainly occur. In more concentrated systems, aggregation is possible, resulting in the formation of clusters, nanoparticles, organometallic compounds and ligand-stabilised mono- and polynuclear complexes of metals and nanoparticles.

Fast spontaneous reactions occurring in the absence of external factors are of greatest interest for cryochemistry of film co-condensates. Such reactions involve consumption of internal energy stored in the film co-condensate; some of them are considered in this review. They proceed by different mechanisms but exhibit an identical kinetics pattern, namely, these are fast (almost explosive) solid-phase low-temperature reactions.

Examples can be found in such reactions as olefin halogenation and hydrohalogenation involving formation of unstable donor–acceptor complexes that prescribe a certain organisation of the reactant molecules, which is necessary to perform the solid-

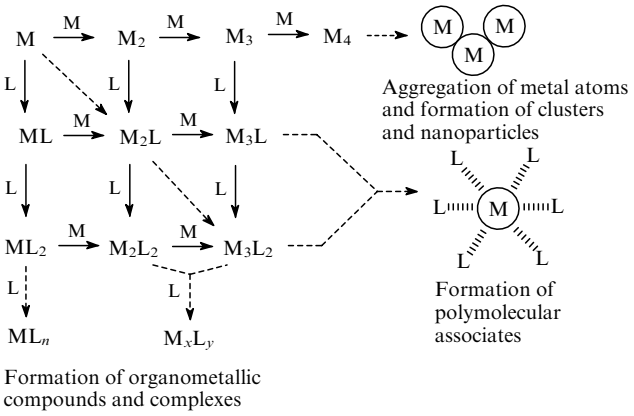


Figure 9. Scheme of successive and concerted reactions proceeding in the course of low-temperature co-condensation of metal (M) and ligand (L) vapours.

phase chemical transformations.[150, 151] No reactions occur in the absence of complexation. This is confirmed by the results of hydrohalogenation of 2-methylbut-2-ene. The reaction rate depends on the extent of complexation in the system 2-methylbut-2-ene – HCl (HCl : olefin = 6 : 1) at 80 K as follows:

Degree of complexation (%)	100	50	0
Conversion (%)			
on co-condensation	39	22	0
on annealing	25	13	0

An explosive reaction was observed in the growing films of magnesium – 1,2-dichloroethane co-condensate[41]

$$Mg + CH_2Cl-CH_2Cl \longrightarrow CH_2=CH_2 + MgCl_2.$$

The reaction products were obtained in nearly 100% yields as the film thickness reaches a critical value (L_c). There is a clear-cut distinction between the reacted and unreacted film regions. Explosive reaction can be accompanied by mechanical fracture of the film. The critical thickness depends on the reactant ratio and on the temperature of the sample. The L_c value is minimum at 1 : 1 $Mg : CH_2Cl-CH_2Cl$ ratio. As the temperature of the sample increases, the region of the explosive reaction becomes more narrow. The reaction is accompanied by fast heat release and crystallisation of the initially amorphous co-condensate film. The process acquires a wave character and the internal energy stored in the co-condensate film initiates explosive reaction. A decrease in the reactant condensation rates and an increase in the temperature of the co-condensate improve the efficiency of relaxation processes in the film, thus making explosive processes less probable. Similar effects were also observed in a study on the reactions of acetyl chloride with diethylamine and cyclopentadiene with titanium tetrachloride.[152] Growth of co-condensate film is accompanied by generation and accumulation of internal strain (excess internal energy) in the sample, which initiates a vigorous reaction and fast crystallisation of the co-condensate after reaching a critical value. Explosive polymerisation reactions initiated by magnesium vapours were observed.[153]

The HCN molecule was found in various space objects, namely, giant clouds of interstellar dust, comets and other galactic objects.[154, 155] It is commonly accepted that the formation of this molecule is a result of one of the main stages of pre-biological chemical evolution, because processes involving HCN can result in amino acids, purines, pyrimidines and other bioactive compounds.[154] Chemical reactions of HCN and its derivatives, *viz.*, cryopolymerisation of HCN and its copolymerisation with acetaldehyde and ethylene oxide as well as polymerisation of cyanogen bromide under conditions similar to those in the interstellar medium (low temperature and initiation by γ-radiation and local brittle fracture) have been studied in detail.[156 – 158]

VI. Cryochemical synthesis and reactions involving metal nanoparticles

Metal nanoparticles of size 1 to 10 nm are of crucial interest for cryochemical research, because in this case small variations of the particle size cause significant changes in their physical and chemical properties. Such objects can be considered as surface structures, because most of the constituent atoms are surface or near-surface ones. An increase in the concentration of uncompensated valence bonds enhances the particles' reactivities.

Main methods for preparation of metal clusters and nanoparticles have been well documented.[159 – 162] Going to low and ultralow temperatures opens up new prospects for production of small metal particles.

Interesting results were obtained using metal evaporation under static pressure of inert gas in the reaction vessel or the inert gas stream technique. A metal can be evaporated by resistive heating and by exposing it to electron or laser beams. Metal clusters and nanoparticles are deposited on internal walls of a reactor or on various substrates.[160] In particular, copper, silver and gold particles of size nearly 10 nm were produced by gas-phase evaporation followed by trapping the freshly obtained particles in frozen liquids (ethanol, methanol and some alkanes).[6, 163] Magnesium particles of size 2 nm were obtained by condensation in liquid helium nanodroplets; larger magnesium particles of size ~100 nm were prepared by condensation in solid argon.[19] Laser evaporation has been employed in studies of almost all metals. For instance, low-energy neutral clusters of iron, cobalt, nickel and nanostructured films of thickness up to 100 nm were produced by deposition on various cooled substrates.[19] Laser and electron beam evaporation of metals are convenient for preparation of bimetallic nanoparticles. A mass spectrometric study of particles formed by co-vapourisation of zinc, cadmium, mercury and sodium revealed the possibility of formation of bimetallic particles comprising one heavy atom surrounded by several (up to 18) sodium atoms.[19] Experiments with sources of ionised cluster beams allowed control of the kinetic energy of the clusters deposited by applying an accelerating potential difference.[164, 165] Gas-phase cluster beams can be size selected and deposited on appropriate substrates. For instance, Pt_n and Pd_n ($n = 1 – 15$) particles were produced on the (100) surface of Ag single crystals.[166]

Novel organometallic clusters and solvated metal nanoparticles are also obtained by condensation of metal vapours.[5, 19] Usually, vapours of metals and organic components are co-deposited on the surfaces of reaction vessels cooled down to 77 – 100 K and lower temperatures. At such temperatures, metal atoms and clusters insert into solid organic matrices. During warm-up of the samples the atoms and small clusters aggregate into large metal clusters and particles of size 10 – 30 nm, which form stable colloidal solutions at room temperature. Further growth of the particles is restricted by solvation and electrostatic effects.

Co-condensation of silver and methyl acrylate vapours on the surface cooled to 77 K followed by heating of the system to room temperature causes partial polymerisation of methyl acrylate and formation of organic colloids comprising silver nanoparticles stabilised by the polymer layer. At room temperature, the optical absorption spectrum of molten co-condensate exhibits a maximum at 400 nm, which is characteristic of spherical silver particles of diameter less than 20 nm.[167] Transmission electron microscopy data indicate formation of silver particles of size less than 15 nm. Co-condensation of silver, lead and methyl acrylate vapours results in colloids of polymer-stabilised bimetallic nanoparticles.[168] The size of lead particles and bimetallic Pb/Ag particles thus obtained is at most 5 nm, which is much smaller than the size of individual silver particles formed under analogous conditions.

Formation of metal nanoparticles during low-temperature co-condensation of silver and 2-(dimethylamino)ethyl methacrylate vapours was studied by optical spectroscopy and dynamic light

scattering.[169] Experimental data as well as the results of electron microscopy investigation of the co-condensates heated up to room temperature indicate initial formation of silver nanoparticles 5 to 12 nm in diameter stabilised in the polymer layer. Low-temperature synthesis of colloidal silver nanoparticles in water, acetone and toluene has also been reported.[170]

Co-condensation of two metals allows preparation of bimetallic core–shell particles. For instance, analysis of Fe/Li co-condensates revealed the presence of particles comprising an iron metal core coated with a $Li_2O/Li_2CO_3/Fe_2O_3$ protective layer.[171] The same approach was employed for the synthesis of bimetallic core–shell nanoparticles in Fe/Mg co-condensates (Fig. 10).[172] These results have first demonstrated the possibility of using cryochemistry for preparation of bimetallic metastable clusters of metals that are immiscible under normal conditions.

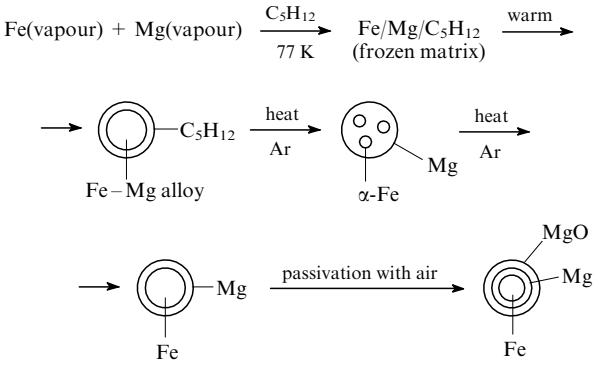


Figure 10. Scheme for preparation of bimetallic core–shell nanoparticles in Fe/Mg co-condensates.[172]

Surface-immobilised metal particles of size 3–8 nm were obtained by impregnating oxide (Al_2O_3, SiO_2, MgO) matrices with molten organometallic co-condensate.[173] Bimetallic particles stabilised on an oxide surface were also prepared by co-condensation of reactant vapours.[174] Colloidal solutions of metal nanoparticles provide an efficient tool for fabrication of nanostructured metallic coatings by solvent evaporation. Such films possess unique properties, *viz*., a higher resistance compared to metal films produced by other methods and the ability to redissolve in appropriate solvents.

Redox reactions on the surface of gold nanoelectrodes, resulting in deposition of the second metal (Pb, Cd, Tl), have been studied.[175] The reactions are initiated by electron transfer from radiolytically generated organic free radicals to the gold nanoparticles rather than application of an external electric field. Because of the large surface area of nanoparticles the reaction can be monitored with a spectrophotometer. Deposition of the second metal causes changes in the size, chemical nature and redox properties of the gold nanoparticles. The physicochemical behaviour of the bimetallic particles thus produced depends on the electronic properties of the adatom layer and on electron exchange at the interface between two metals with different electron work function.

Bukhtiyarov and Slin'ko reported a comprehensive review on the properties of metal nanoparticles stabilised on solid surfaces.[176] They analysed the reactivities and selectivities of metal particles in relation to particle size and to the atomic and electronic structure of bulk metals. This allowed consideration of the properties of metal clusters and nanoparticles and of the active sites of heterogeneous catalysts in the framework of a unified approach.

Studies on the reactivity of metal nanoparticles over a wide temperature range revealed novel unusual chemical reactions. Namely, silver nanoparticles encapsulated into poly(*p*-xylylene) films possess catalytic activity in the reaction of methanol oxidation into formaldehyde, silver nanoparticles stabilised on an alumina surface catalyse epoxidation of ethylene[7] while the reaction of zinc nanoparticles with CCl_4 in water causes an increase in the rate of dechlorination and results in methane.[177]

VII. Assembly of hybrid nanostructures at low temperatures

Novel technologies widely use nanoscale hybrid materials (organic compound–metal; metal–semiconductor; metal–dielectric) that are stable at room temperature.[178] These materials are characterised by large interface areas and extended boundaries between different structural elements. Interactions of such nanoscale structures with photons and electrons cause manifestation of unusual optical, magnetic and electrophysical properties.[179, 180] The properties of individual nanoparticles and nanostructured films, methods for their preparation, self-organisation of nanoparticles, growth of oriented nanoscale films and template synthesis of nanoparticles have been reviewed.[27–33] In the text below we present some examples of preparation of these materials using cryochemical techniques.

1. Low-temperature condensation and surface reactions

Various hybrid nanostructures were fabricated by condensation of atom-molecular beams on cooled dielectric, semiconductor and metal surfaces. For instance, multilayer dinitrogen films adsorbed on a graphite surface were studied at 12–20 K.[181] This allowed determination of the tilt angles of the molecular axes with respect to the graphite surface and establishment of two main types of molecular packing within the layer with an increase in the surface coverage from submonolayer to formation of a bilayer structure. Detailed neutron diffraction studies on the growth mode of methyl chloride (CH_3Cl), dichloromethane (CH_2Cl_2) and chloroform ($CHCl_3$) condensate films on a graphite surface have been reported.[182, 183]

Monolayers of long-chain saturated hydrocarbons were adsorbed on the Cu(111) surface cooled down to 80–160 K.[184] At low temperatures, octane forms a commensurate crystal lattice and undergoes a first-order phase transition on heating. Nonane forms a domain surface structure with parallel arrangement of molecules and experiences an unusual, strongly broadened phase transition on heating. This is consistent with the known odd–even effect observed in the structures of solid alkanes. Whereas alkanes C_nH_{2n+2} with even n values have structures with monoclinic or triclinic unit cells, odd-numbered alkanes have an orthorhombic unit cell. These organic layers adsorbed on metal surfaces can be used in molecular electronics and optoelectronics.[185–187] Electron transfer in structured layers of hexafluorobenzene and phenylthiol on the Cu(111) surface has been studied.[188] The interaction between organic molecules and the surface layer of the metal crystal affects charge transfer across the interface.

Ultrathin gold films were prepared by low-temperature condensation on a silicon surface at 173–300 K.[189] It was found that the surface of the silicon crystal and the pure metal layer are separated by a layer of amorphous gold silicide 13–28 Å thick.[190] A study of 0.3 nm silver films deposited on the Si(111), Si(100) and Ge(001) surfaces at 100–300 K revealed formation of ordered 2D structures,[191] which are assigned to the most promising objects for creation of a novel class of 2D superconductors with $T_c = 2–8$ K.[191] As the thickness of the silver layer increases, island 3D structures are mainly formed. Cold-deposited silver thin films exhibited second harmonic generation.[192] Analysis of the results obtained confirmed a homogeneous structure of the deposited 3D silver films of thickness 15–20 nm. Lead films prepared by depositing Pb on the Si(111) surface provide the most convenient system for analysing various effects in the absence of interdiffusion and chemical reactions.[193] The Schottky barrier to a Pb/Si diode depends on the structure of the near-surface layer at the interface. Using surface X-ray diffraction, it was shown that growth of initially amorphous film is followed by

its crystallisation to well-ordered Pb(111) structures after reaching a critical thickness of 5 atomic Pb layers. Layer-by-layer deposition at 100 K allows suppression of the growth of 3D island structures.

Interfacial bimetallic systems formed by deposition of adatoms of the second metal on the crystal surface of the major metal component are of considerable interest.[194–196] Catalytic activity of such systems has long been known; however, reliable investigation techniques were developed only in the last decade. Condensation of adatoms on metal surfaces at 100–200 K eliminates all types of mobility, except for surface diffusion during the film growth. Specific features of nucleation and the kinetics of formation of layer-by-layer deposited surface monolayers and island films as well as the growth of bulk 3D phases are first of all determined by close values of the lattice parameters of the two metals, by the ability to form bimetallic compounds and alloys, by strain in the growing film and by the relaxation mechanism of excess elastic energy. The lifetime of the adatom in the excited state and the electron states of the metal surface at low temperatures can be studied by time-resolved two-photon photoemission spectroscopy.[197] It was established that ternary hybrid metal nanostructures Cu/Co/Cu(001), Pd/Co/Pd(001) and Fe/Cu/Fe(001) possess unusual magnetic properties including magnetic anisotropy and tunnelling magnetoresistance. Substances exhibiting these properties can be used as magnetic sensors and magnetic recording systems.[198] Deposition of metal atoms and clusters on an oxide surface is of particular interest because this technique allows preparation of size-selected metal particles and modelling of the efficiency and selectivity of catalysts.[199, 200]

The vapour deposition technique allows controlled condensation of atoms and clusters on various surfaces by thermal or photochemical decomposition of precursor vapours.[201] Controlled adsorption and decomposition of iron pentacarbonyl, chromium hexacarbonyl and cyclopentadienylrhodium dicarbonyl on the single-crystal surfaces of Ag, Pt, Au and Cu at 80–300 K were studied by reflection absorption IR spectroscopy.[202, 203] Photodissociation of neutral molecules on cold surfaces of various metals was studied; some examples are provided by the CH_3I/Cu(110),[204] Bu^tNO_2/Ag(111)[205] and NH_3/Pt(111), Ge(100), Si(100) pairs.[206, 207]

Yet another promising method of cryochemical research, which allows preparation of hybrid nanostructures, involves the action of aggressive gases on the surface of metal crystals at low temperatures. Chlorination of different crystallographic planes of silver and copper single crystals has been studied.[208] A 2-nm thick metal chloride layer is formed upon exposure of the Ag(111) surface to chlorine gas at 150–250 K. Thin layers of silver and copper chlorides can be used for fabrication of nanocrystalline materials (metal clusters dispersed in the bulk of the chloride phase: Ag_x/AgCl and Cu_x/CuCl). Local oxidation of titanium, aluminium and copper surfaces was performed by exposing them to an oxygen stream accompanied by scanning the corresponding local area with the probe tip of a scanning tunnelling microscope. By applying an appropriate potential difference between the surface and the probe tip and moving the probe tip across the specified surface area it is possible to 'draw' metal oxide lines 10–20 nm thick (Fig. 11).[209] A local nanoscale etching technique was also used for modification of the surface of a silicon crystal.[210] Nanoscale silicon rods on the surface treated were prepared by nitration and subsequent oxidation of the surface monolayer. Efficient etching of the Si(111) surface by thermalised hydrogen atoms was performed at 105 K.[207, 211] The products obtained, silanes and disilanes, were removed from the surface by heating the samples to 480 K.

Silver, copper and platinum crystals are good catalysts of oxidation processes. However, organic molecules are poorly adsorbed on their surfaces at temperatures above 150 K. The situation changes in the presence of adsorbed oxygen.[212] Efficient low-temperature oxidation of cyanogen $(CN)_2$, carbon monoxide, ethyl iodide, methanol, nitrobenzene and styrene molecules on the

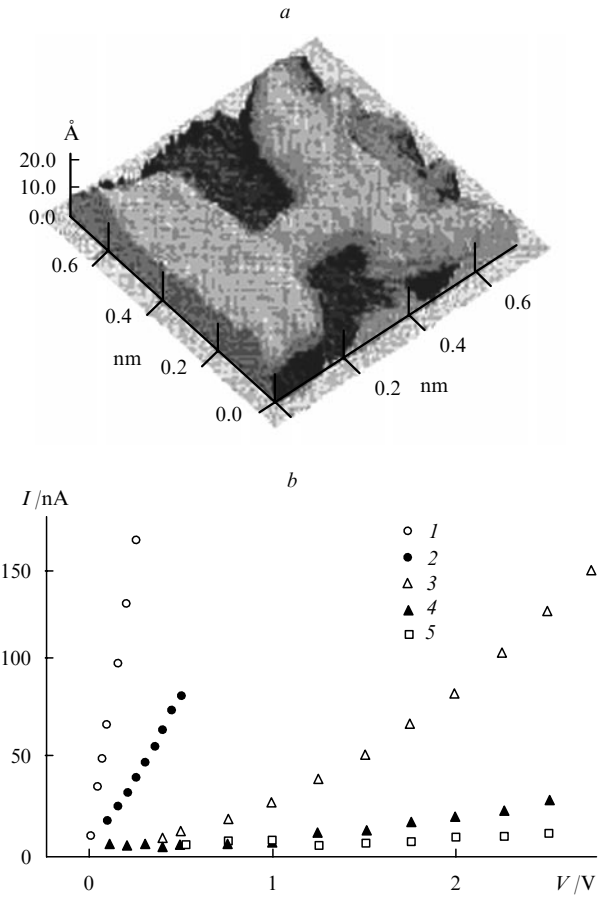


Figure 11. AFM image of crystalline titanium surface after nanoscale local oxidation by simultaneous action of oxygen and the probe tip of a tunnelling atomic force microscope (*a*) and the current-*vs*.-voltage curves for the system at different temperatures (*b*).[209]
T /K: 250 (*1*), 190 (*2*), 130 (*3*), 90 (*4*) and 77 (*5*).

Ag(110), Pt(113) and Cu(110) surfaces was carried out in the presence of adsorbed oxygen.[213–215]

The most important oxidation processes in the environment and in living organisms involve dioxygen. They can also retain selectivity at low temperatures as, *e.g.*, industrial catalytic processes involving C_1-molecules on gold-containing catalysts. A complete catalytic cycle for the transformation

$$CO + 1/2\,O_2 \longrightarrow CO_2$$

on gold cluster anions Au_N^- is illustrated by Fig. 12. The reaction exhibits nonmonotonic cluster-size dependences of the amount of adsorbed carbon oxide and of the conversion efficiency (Fig. 13). This reflects improved stabilities of nanoclusters with closed outer electron shells ($N = 8$, 14, 18 and 20).[216–218]

Dissociative adsorption of methane on the surface of Ni single crystals was considered as a model for reforming on small nickel crystallites dispersed in a highly porous Al_2O_3/MgO matrix.[219] Reactions of hydrogen atoms with acetone on graphite monolayers coated on the Pt(111) surface were studied by high-resolution electron energy loss spectroscopy and thermal desorption spectroscopy at 90 K.[219]

2. Polymer films containing metal nanoparticles

Low-temperature vacuum codeposition of metal (Ag, Mg, Cd, Zn, Pb, Sm, Sn, Mn) vapours with *p*-xylylene, which polymerises at low temperatures (100–120 K), was employed to prepare metal nanoparticles ($d = 5$–10 nm) encapsulated into polymer films.[220–227] Polymerisation at cryogenic temperatures and formation of the polymer network preclude subsequent aggregation

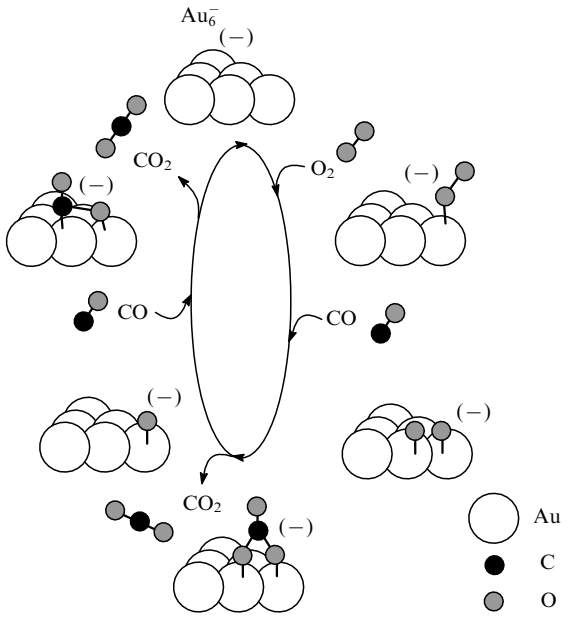


Figure 12. Scheme of complete catalytic cycle for conversion $CO + 1/2\,O_2 \rightarrow CO_2$ on gold clusters Au_N^- (see Ref. 216).
N is the number of atoms in the cluster.

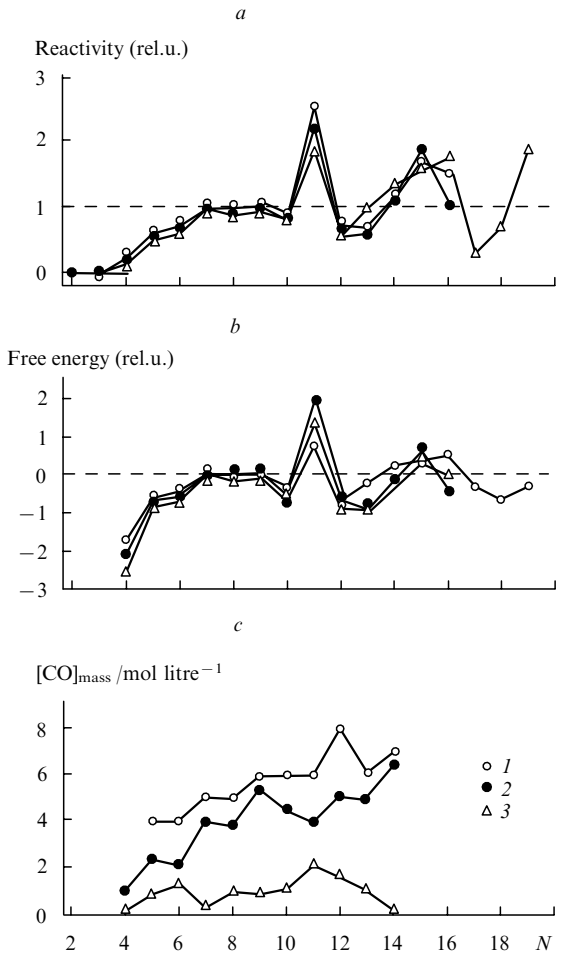
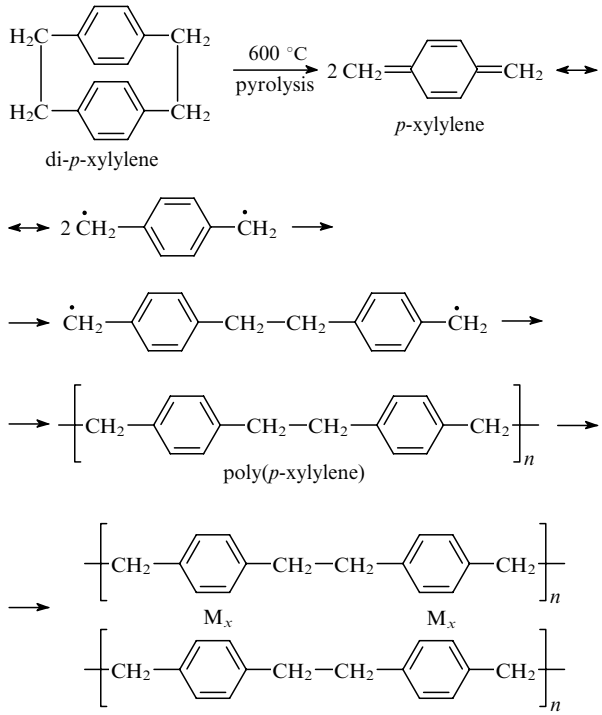


Figure 13. Dependences of the reactivity (*a*), free energy (*b*) and amount of adsorbed carbon oxide (*c*) on the size of Au_N^- clusters at different exposure times in CO (*1–3*).[216]

of the metal particles. Poly-*p*-xylylene films containing encapsulated metal nanoparticles can be separated at room temperature and investigated by various spectral and physicochemical methods. The following scheme of cryochemical synthesis of poly(*p*-xylylene) films containing nanoscale metal particles (M) was proposed:



The films obtained were studied by transmission electron microscopy and X-ray diffraction. The content of metal in the samples was determined by X-ray fluorescence analysis. It was found that globular lead particles are homogeneously dispersed in the film (Fig. 14). The average particle size was 5.5 nm, being independent of the metal content in the film from 0.1 to 6.5 mass %. The particles were treated as crystals.[224] The lattice parameters of the zinc and cadmium particles encapsulated into poly(*p*-xylylene) films were in good agreement with the lattice parameters of bulk metals. Exposure of the films to oxygen over a period of several days led to formation of new metal-oxide crystalline phases ZnO and CdO.[224]

Poly(*p*-xylylene) is a typical insulator. Encapsulation of lead nanoparticles into the film (up to 10% by mass) has no effect on the material's characteristics, the resistivity of the films is $10^{16}\ \Omega\ cm^{-2}$ (see Ref. 225). Changes in the conductivities of the

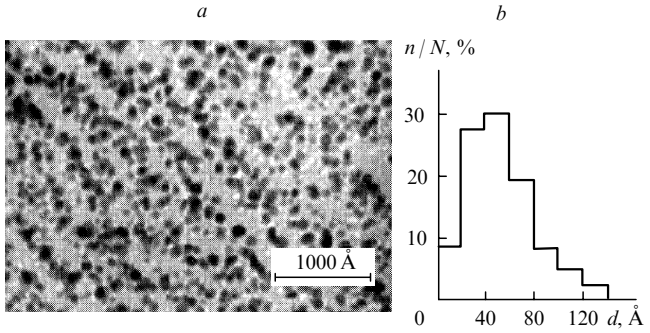


Figure 14. Electron micrograph (*a*) and size distributions (*b*) of lead particles stabilised in poly(*p*-xylylene) films ([Pb] = 6.5 mass %);[224]
n is the number of nanoparticles of a given size and *N* is the total number of nanoparticles.

samples were studied during low-temperature co-condensation of vaporous components and on heating of the samples in the temperature range 80–300 K.[225] Polymer films containing nanoscale lead particles exhibit activity as gas and vapour sensors towards various organic and inorganic substances.[226–230] The conductivity of the film samples varies by four to six orders of magnitude.

3. Hybrid metal–mesogen nanosystems

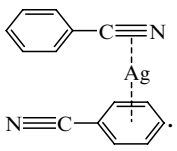
Ordered nanoscale structures are of considerable interest because of unusual physical and chemical properties. The use of liquid crystals as self-organising organic matrices opens up new prospects for the synthesis of anisotropic metal nanoparticles and their compounds and for fabrication of organised ensembles of nanorods and nanowires based on them.

Silver-containing cyanobiphenyl films were prepared by vacuum co-condensation of vaporous components on cooled CaF_2, quartz and copper surfaces.[231–233] Silver/4-alkyl-4′-cyanobiphenyl co-condensate samples were studied by EPR, IR and UV-visible spectroscopies in the temperature range 80–350 K and by transmission electron microscopy at room temperature. The spectral features observed were analysed using the results of model quantum-chemical calculations of the equilibrium structures and vibrational analysis.[234]

Spectroscopic studies of binary Ag/CB co-condensate films with the component ratio varied from 1 : 1 to 1 : 100, as well as investigation of ternary Ag/CB/decane co-condensate films at 90 K revealed the presence of metastable complexes formed as a result of interaction between silver atoms and cyanobiphenyl molecules. In particular, the IR spectra of the Ag/5CB co-condensates exhibited two new bands at 2080 and 2030 cm^{-1} in the region of CN stretching vibrations (see Ref. 231). These bands are shifted by -150 and -200 cm^{-1}, respectively, with respect to the corresponding band of 5CB (2230 cm^{-1}). The observed decrease in the stretching vibration frequencies indicates the formation of a silver–cyanobiphenyl π-complex. Indeed, partial donation of electron density from the bonding orbital of silver to the ligand antibonding orbital should cause elongation of the multiple bond in the complex and, hence, a decrease in its vibrational frequency. The frequency shifts by 100–200 cm^{-1} towards the low-frequency region were observed in a study on π-complexation of some transition metals with unsaturated compounds.[235] The spectra of the Ag/5CB and Ag/5CB/$C_{10}H_{22}$ co-condensates also exhibited a new band in the region 650–660 cm^{-1}, which was assigned to the vibrations of the metal–ligand bond in the π-complex Ag(5CB). Similar results were obtained for co-condensates of silver with 8CB and 4-octyloxy-4-cyanobiphenyl (8OCB). In both cases the intensities of the IR bands of π-complexes changed with the co-condensate temperature following an identical pattern. Because of this, the bands were assigned to the same complex. Complexes Ag(CB) are stable at low temperatures and decompose on heating of the co-condensates to 200–300 K into starting CB and silver clusters. At room temperature, the IR spectrum of Ag/CB co-condensate is similar to that of the CB condensate film. The results obtained are consistent with the low thermal stabilities of the complexes of zero-valence metals with unsaturated compounds.

The formation of π-complexes in the system under study was confirmed by the results of quantum-chemical calculations of 5CB and of the central cyanophenyl fragment of the complex.[234] The calculations were carried out by the multiconfiguration self-consistent field method and by the restricted Hartree–Fock method for open-shell systems. The Stevens–Basch–Krauss effective core pseudopotential was employed for all heavy atoms. Both geometry optimization of and vibrational analysis for the (PhCN)Ag, $(PhCN)Ag^+$ and $(PhCN)Ag_2$ particles have demonstrated that global energy minima for these systems correspond to σ-complexes with linear arrangement of the C—N···Ag fragment. The shifts of the C—N stretching vibration frequencies in the complexes relative to the corresponding value for the ligand molecule were $+9$, -7 and $+20$ cm^{-1} for the equilibrium N···Ag distances of 2.81, 2.24, and 2.46 Å, respectively. Therefore, the calculated configurations do not correspond to real structures in the Ag/5CB films since the experimentally observed shifts of the CN stretching vibration frequency are -150 and -200 cm^{-1}.

At the same time liquid-crystalline cyanobiphenyls are known to form dimeric structures in the solid and liquid-crystalline phases. Structural studies[236,237] showed that cyanobiphenyl molecules in the solid phases are arranged in the 'head-to-tail' manner. Based on this, the following structure of the silver–cyanobiphenyl complex was proposed (shown is the central part of the complex):



The cyano groups in this structure are nonequivalent and give two bands in the IR spectrum of the complex.

Multiconfiguration self-consistent field calculations revealed the possibility of two ground-state electronic configurations of the complex, $(PhCN)_2Ag$ and $(PhCN)_2^-Ag^+$.[234] At long interligand distances R ($R \geqslant 4.7$ Å), neutral silver atoms fill the interligand cavities. At $R < 4.7$ Å, the charge-transfer configuration $(PhCN)_2^-Ag^+$ dominates. If $R = 4.4$ Å (a charge-transfer complex), the calculated shifts of the C—N vibrational frequencies in the $(PhCN)_2Ag$ complex relative to the corresponding value for the PhCN molecule (2501 cm^{-1}) were found to be -150 and -175 cm^{-1}, which is in agreement with the experimentally observed shifts for the Ag/5CB films at 90 K.

Thermal behaviour of the metal-containing atom–molecular systems based on co-condensates of silver and mesogenic cyanobiphenyl 5CB was investigated in the temperature range 80–300 K.[233] At 80 K, the EPR spectra of the co-condensates exhibited well-resolved signals of hyperfine coupling (HFC) with the metal atoms. This indicates formation of complexes between silver atoms and mesogenic ligands under conditions of low-temperature co-condensation. The parameters of the doublets, obtained by simulating the spectra of the Ag/5CB and Ag/5Py co-condensates are characteristic of π-complexes of the ^{107}Ag ($J = 1/2$) and ^{109}Ag ($J = 1/2$) atoms. By comparing the HFC constants of the complexes with those of free atoms [$A(^{107}Ag) = 611$ and $A(^{109}Ag) = 705.4$ G][46] it is possible to estimate the unpaired s-electron density on the metal atom: $\rho_s = 0.89$ (Ag/5CB). The central signal in the region characteristic of the g-factor of a free electron is due to absorption of the silver clusters stabilised in the 5CB matrix. Similar signals were observed for concentrated samples of co-condensates of silver with inert gases and hydrocarbons. They were treated as the spin resonance signals of conduction electrons in the metal nanoclusters. The average size of silver clusters in the Ag/5CB co-condensate (Ag : 5CB = 1 : 10) estimated from the experimental spectrum recorded at 90 K is 1–2 nm (several tens of atoms). Raising the temperature from 80 to 150 K causes a decrease in the relative intensities of the doublets in the spectrum and an increase in the relative intensity of the central component, which indicates thermal degradation of the complex and the growth of silver nanoclusters. The possibility of formation of silver nanoclusters by UV irradiation of samples at 80–90 K was demonstrated.[238] Heating of such samples above 200 K also causes a rapid decrease in the intensity of the central line in the EPR spectra and the appearance of a broad background absorption, which can be explained by the formation of larger silver nanoparticles and their aggregates.

At 90 K, the optical absorption spectra of Ag/5CB co-condensates exhibited[233] a structured band at 360 nm. Quantum-chemical calculations of excited states of the complex revealed a number of intense transitions corresponding to

metal – ligand and ligand – ligand charge transfer in this region.[239] It should be noted that small clusters of silver can also absorb in the region 390 – 420 nm.[37] The structured band at 360 nm disappears on heating of the co-condensate film to 200 – 300 K.[234] Thus, heating of the sample to room temperature causes thermal degradation of the complex and aggregation of the silver atoms thus released. The broad band with a maximum at 440 nm which appeared in this case is due to absorption of surface plasmons of nanoscale silver particles[240] that are formed as a result of aggregation of silver atoms upon decomposition of the complex. Fast heating of the co-condensate to 300 K causes a transition of the sample to the nematic mesophase. This is followed by an increase in the absorption of the plasmon resonance in the long-wavelength region of the UV spectrum, which can be due to both the growth of silver particles due to further aggregation and the formation of non-spherical anisotropic metal particles in the orientationally ordered matrix.

Thus, the sample prepared by low-temperature co-condensation of the metal (silver) and mesogenic component vapours and heated to room temperature is a material containing silver nanoparticles stabilised in the cyanobiphenyl matrix.[240] The material retains nematic properties. The samples obtained and the pure 5CB are characterised by an identical thermogram pattern and by textures typical of the nematic phase.

Low-temperature layer-by-layer co-condensation of silver, 5CB and *p*-xylylene vapours followed by heating of the film sample results in encapsulation of the metal – mesogen system into the polymer film.[240] An electron microscopy study of the films prepared by encapsulating silver-containing 4-pentyl-4′-cyanobiphenyl into poly(*p*-xylylene) under conditions of vacuum co-condensation of reactants revealed the presence of two types of metal particles stabilised in the mesogenic matrix at room temperature.[240] These are globular silver particles of diameters 15 to 30 nm and anisotropic rod-like particles more than 200 nm long (Fig. 15). The UV spectrum of the Ag/5CB films in poly(*p*-xylylene) exhibits a broad absorption band at 440 – 600 nm at room temperature. An increase in the metal-to-ligand ratio in the sample causes a preferred growth of rod-like silver particles.

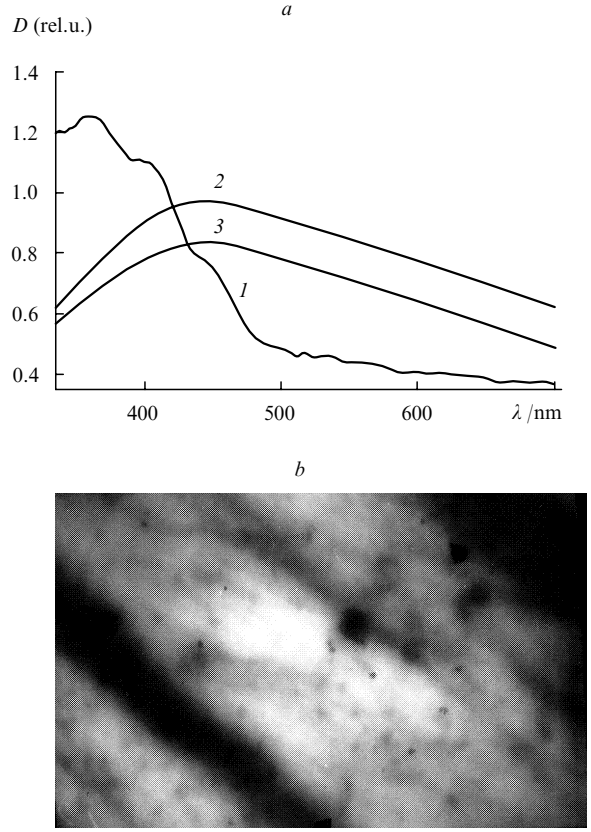


Figure 15. Optical absorption spectra of a Ag/5CB (Ag : 5CB = 1 : 10) co-condensate film at 90 (*1*), 200 (*2*) and 300 K (*3*) (*a*) and an electron micrograph of the film at 300 K (*b*) (1 cm = 100 nm).[240]

Thus, silver-containing mesogenic cyanobiphenyl films prepared by low-temperature co-condensation of component vapours (molecular beam regime) incorporate metastable π-complexes of the metal with dimeric cyanobiphenyl molecules. The formation of metastable π-complexes in the temperature range 90 – 200 K was confirmed by EPR, IR and UV spectroscopies and by the results of quantum-chemical calculations of a model silver – cyanophenyl system. Raising the temperature causes degradation of thermally unstable complexes and aggregation of silver atoms in the anisotropic liquid-crystalline matrix, resulting in silver nanoclusters and nanoparticles. Thermal and photo-induced decomposition of the complexes in the temperature range 90 – 200 K is accompanied by the formation of nanoscale silver clusters and further aggregation of these species in the anisotropic matrix. The formation of globular metal particles (15 – 30 nm) and anisotropic metal – mesogen nanostructures including rod-like aggregates more that 200 nm long stabilised in the cyanobiphenyl matrix was established.

4. Nanoparticle ensembles and superlattices

Recently, intensive research on preparation and self-assembly of nanoparticles on various surfaces has been carried out.[241, 242] These investigations are aimed at finding possible applications of surface nanostructures and nanostructured films in various nanoelectronic data recording and processing devices, optical and magnetic filters, displays, switches, *etc*.

Silver and gold nanoparticles are convenient for studying self-assembly effects. Periodic structures are formed immediately in colloidal solutions of gold and silver nanoparticles stabilised by a variety of thiol- and nitrogen-containing ligands[125, 243] and on various surfaces modified with amines and thiols.[244] Formation of alternating positively and negatively charged gold and silver nanoparticles and their organisation into ordered structures on glass surfaces in the presence of 4-aminothiophene and 4-carboxythiophene was observed.[245] Detailed analysis of the stabilisation of the metal nanoparticles by ligands and of their organisation into periodic 1D, 2D and 3D structures has been reported.[246]

Self-assembly of spherical gold nanoparticles 2 – 5 nm in diameter into rod-like aggregates has been studied.[247] It was shown that the size, shape and morphology of aggregates can be controlled by varying the substrate temperature. For instance, the species prepared were spherical aggregates of particles of diameter 97 ± 17 nm (23 °C), spherical particles of size 0.5 – 1 μm (−23 °C) and nearly 50-nm long chain-like 1D aggregates comprised of spherical units (intermediate temperature, 10 °C). It was assumed that the formation of large globular aggregates from small spherical particles involves an intermediate stage in which linear aggregates are formed and that this stage is controlled by the enthalpy-to-entropy contribution ratio. Orientationally ordered gold nanorods were prepared.[247] Using femto- and nanosecond lasers, nanorods were reversibly transformed into spherical nanoparticles.

Self-assembly of Sb_4 clusters on the surface of highly ordered pyrolytic graphite or molybdenum disulfide was studied.[248] The evolution of the structure and morphology pattern of the particles with an increase in the surface coverage was studied by electron microscopy and electron diffraction (Fig. 16). It was found that amorphous spherical nanoparticles are formed at low surface coverages. After reaching a critical size of 120 nm (at room temperature), finger-like island and planar 2D structures were formed. Well-shaped, orientationally ordered 3D nanocrystals

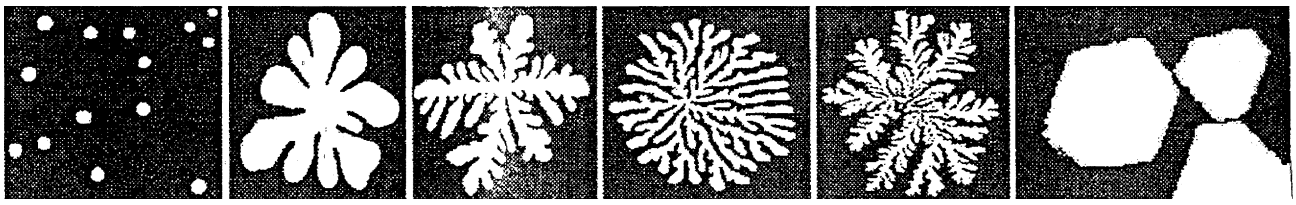


Figure 16. Evolution of the morphology pattern of antimony nanoclusters Sb_4 on the surface of highly ordered pyrolytic graphite with an increase in the surface coverage (from left to right) according to electron microscopy data.[248]

with narrow size distribution grew with increasing surface coverage. Thus, the authors of this study observed a size-dependent structural phase transition from the amorphous to the crystalline state. An analogous transition was earlier observed in the formation of gold nanocrystals by deposition on a graphite surface[249] and ice crystals from amorphous supercooled water vapour.[250] The phase transition observed depends on the condensation rate, surface coverage and the temperature of the sample.

The influence of the nature and surface morphology of the substrate (pyrolytic graphite or molybdenum disulfide) on the formation of ordered 2D and 3D superlattices was observed taking dodecanethiol-stabilised silver nanoparticles of diameter 5.8 nm as examples.[251] Control of substrate morphology is of great importance for pharmaceutical and food-industry applications.[252] For instance, self-assembled organothiol monolayers on the Au(111) surface were used as templates for the growth of glycine crystals.[252] Highly ordered styrene structures on the Si(100) surface were produced by scanning the corresponding local areas with the probe tip of a scanning tunnelling microscope. By modifying the silicon surface it is possible to change the orientation and length of molecular arrays on the surface, control their direction and vary the angle of chain propagation.

Self-ordering of alkanethiol monolayers on the surface of gold nanoparticles has been reported.[253] Introduction of fluorocarbon substituents improves the stability of the ordered layers. Their thermal stability increases with an increase in the number, n, of methylene groups in the organic stabiliser molecule. At $n = 33$, the ordered films do not experience thermal degradation at 150 °C for 1 h in air. Gold nanoparticles stabilised by fluoroalkyl ligands can form hexagonal close-packed and cell structures.[254] The type of ordering is primarily determined by the nanoparticle size ratio and by steric hindrance produced by the stabilising ligands. Stable nanosystems comprising gold particles ($d = 4$ nm) incorporated into polyethyleneimine and poly(L-lysine) films and additionally stabilised by carboxylic acids were obtained.[255]

Monolayers of ordered 2D structures comprised of ligand-stabilised nanoparticles can be used as selective chemoresistive sensors for volatile organic compounds. In particular, ordered 2D structures formed in monolayers of gold nanoparticles stabilised by alkanethiol ligands (Fig. 17) are highly sensitive to toluene, tetrachloroethylene, propan-1-ol and water vapour.[256] Ordered thin-film surface structures built of functionalised organic molecules specifically bound to the surfaces of metallic and polymeric substrates also exhibit the properties of selective sensors. As an example, Fig. 18 presents a scheme of organisation of resorcin-[4]-arene monolayers that are covalently bound to the Au(111) surface and can selectively bind various organic molecules ($CCl_2=CCl_2$, $CCl_2=CHCl$, CCl_4 and toluene).[257]

Highly ordered organic monolayers adsorbed on the surface of inorganic nanoparticles can be used for selective binding of various functional blocks to organise hybrid nanostructures. This can be done using, *e.g.*, biomacromolecules. In particular, the ability of peptides and DNA molecules to show molecular 'recognition' can be modelled using relevant synthetic analogues. Recent advances in molecular biology allowed one to obtain natural and synthetic biomolecules, which can selectively bind metal and metal oxide particles. There are two approaches to exploiting biomolecules as the 'glue' for different inorganic blocks.[257] The first involves mutual organisation due to 'programmed' interaction between biomolecules with the known 'recognition' mechanism. In this case, the hybrid material is generated from two different inorganic blocks modified with molecules of peptides, antibodies, oligonucleotides or other bioligands complementary to one another. The second strategy involves specific interactions between inorganic blocks bearing particular functional groups and the bifunctional biomolecule. Recently, this approach was implemented practically.[258]

Nanostructured surfaces prepared by deposition of size-selected metal clusters and nanoparticles can be used for selective binding and immobilisation of particular biomolecules. Such systems are promising for fabrication of sensitive biochips. For instance, by depositing size-selected gold clusters onto graphite surfaces it is possible to create stable organised structures for selective binding of such practically important biomolecules as peroxidase and DNA.[259–260] This method also permits optical detection of individual biomolecules bound to the nanoparticle surface.[261]

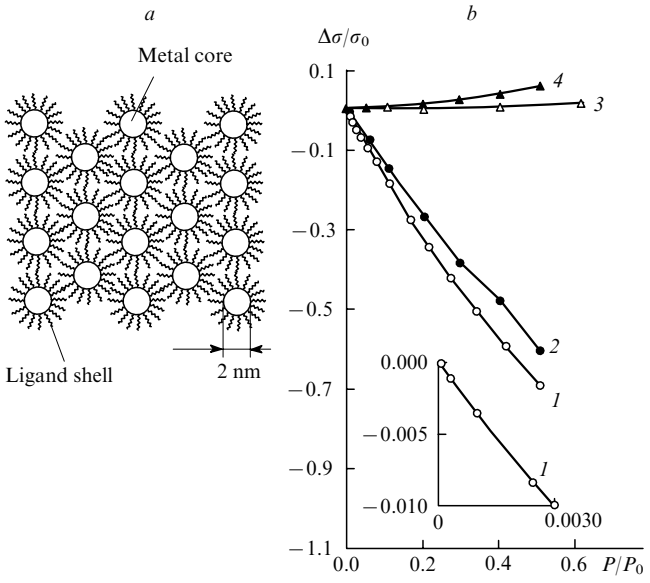


Figure 17. Ordered 2D structures formed in monolayers of gold nanoparticles stabilised by alkanethiol ligands (*a*) and their sensitivity to toluene (*1*), tetrachloroethylene (*2*), water (*3*) and propan-1-ol (*4*) vapours (*b*);[256]
$\Delta\sigma/\sigma_0$ is the relative change in the layer conductivities; P/P_0 is the ratio of the partial vapour pressure of the organic compound to the total pressure in the system.

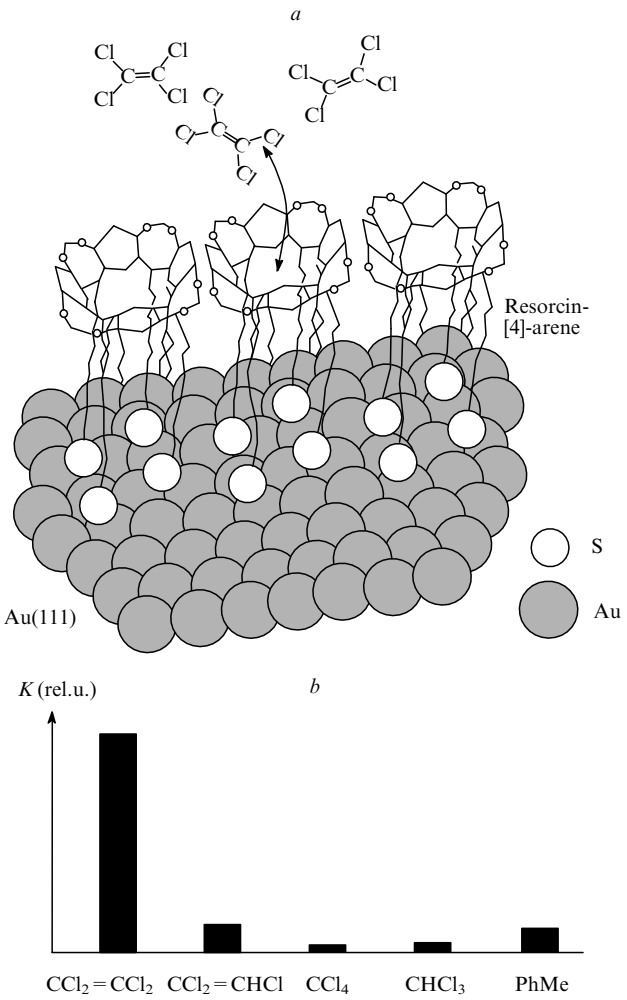


Figure 18. A scheme of organisation of resorcin-[4]-arene monolayers covalently bound to the (111) surface of gold single crystals and capable of selective binding of various organic molecules (*a*) and binding selectivity diagram for these molecules (*b*);[257]
K is the binding constant.

VIII. Conclusion

Cryochemistry allows one to investigate highly reactive particles, atoms, clusters, metal nanoparticles and their organised ensembles. At cryogenic temperatures, chemical interactions begin at the atomic level. Co-condensation and subsequent warm-up of samples are characterised by competition between aggregation and stabilisation of atoms and small clusters in matrices. Introduction of complexing ligands and reactive species into the system causes additional chemical and physicochemical processes resulting in unusual chemical compounds and complexes. Aggregation of atoms and their interaction with ligands occur almost barrierlessly. High reactivities of metal atoms, clusters and nanoparticles preclude establishment of correlations between the particle sizes (number of atoms in the particle) and their reactivities. This problem, as well as the problems of synthesis and stabilisation of atoms, clusters and nanoparticles can be solved only by carrying out spectroscopic studies at cryogenic temperatures.[262] Based on the results obtained thus far, the size of the reacting particle can be considered as a parameter which determines the state and chemical properties of a reaction system along with the temperature.[263]

At cryogenic temperatures, processes occur under strongly nonequilibrium conditions in metastable systems characterised by a broad reactivity distribution of the reacting species. This manifests itself as peculiar features of the kinetics of low-temperature processes.

Operation at cryogenic temperatures allows preparation of small particles of size less than 1 nm. Potential applications of such species are related to the search for highly efficient stabilisers of nanoparticles. Novel catalysts and sorbents, optical and anticorrosive coatings, pharmaceuticals and dyes, degassing agents and bioactive components can be prepared at cryogenic temperatures. High reactivities of small stabilised particles make it possible for them to be considered as chemical systems for energy accumulation and storage and as specific nanoscale chemical reactors. Such systems allow the carrying out of novel chemical reactions and unusual chemical transformations, which cannot proceed under normal conditions.

Currently, efficient cryochemical methods for stabilisation of nanoparticles in matrices and on various surfaces and procedures for fabrication of nanostructured film materials with prescribed optical, magnetic, electrophysical and mechanical characteristics are being developed. The future of these approaches is closely related to extension of the field of possible practical applications of nanosystems in nanotechnologies.[264, 265] These are primarily creation of toxic gas sensors, highly selective and reactive catalytic systems, membranes and highly porous sorbents with large surface areas and prescribed pore sizes, novel ultrahard and superplastic materials, coating-protective nanoalloys, absorbing and reflecting ceramics, pharmaceuticals with improved bioavailability and controlled delivery, novel hybrid organometallic materials and bio-metalloceramic composites.

This review has been written with financial support from the Russian Foundation for Basic Research (Project Nos. 99-03-32206, 00-03-32944, 02-03-32469) and the 'Russian Universities' Programme.

References

1. M Moskovits, C A Ozin (Eds) *Cryochemistry* (New York, London, Sydney, Toronto: Wiley, 1976)
2. G B Sergeev, V A Batyuk *Kriokhimiya* (*Cryochemistry*) (Moscow: Khimiya, 1978)
3. G B Sergeev, V V Smirnov *Molekulyarnoe Galogenirovanie Olefinov* (Molecular Halogenation of Alkenes) (Moscow: Moscow State University, 1985)
4. G B Sergeev (Ed.) *Modern Trends in Low Temperature Chemistry* (Moscow: MSU-Press, 1994)
5. K J Klabunde, in *Free Atoms, Clusters and Nanoscale Particles* (San Diego: Academic Press, 1994) p. 311
6. K Kimura *Bull. Chem. Soc. Jpn.* **60** 3093 (1987)
7. G B Sergeev, in *Khimicheskaya Fizika na Poroge XXI Veka. K 100-letiyu Akademika N N Semenova* (Chemical Physics at the Threshold of the XXIst Century. Academician N N Semenov Centenary Anniversary) (Moscow: Nauka, 1996) p. 149
8. G B Sergeev *Usp. Khim.* **70** 915 (2001) [*Russ. Chem. Rev.* **70** 809 (2001)]
9. L Andrews, M Moskovits (Eds) *Chemistry and Physics of Matrix-Isolated Species* (New York: Elsevier, 1989)
10. M A Almond, A J Downs *Spectroscopy of Matrix-Isolated Species* (New York: Wiley-Interscience, 1987)
11. L Khriatchev, M Petterson, N Runebera, J Lundell, M Rasanen *Nature (London)* **406** 874 (2000)
12. L Khriatchev, I Lundell, H Tanskanen, M Patterson, M Rasanen, J Ahokas, H Kunttu, V Feldman *J. Chem. Phys.* **116** 5649 (2002)
13. B L Grigorenko, A V Nemukhin, V A Apkarian *J. Chem. Phys.* **104** 5510 (1996)
14. G M Chaban, J Lundell, R B Gerber *J. Chem. Phys.* **115** 7341 (2001)
15. E G Baskir, V A Korolev, O M Nefedov *J. Mol. Struct.* **480–481** 519 (1999)
16. G A Gurgis, S Bell, C Zheng, J R Durig *Phys. Chem. Chem. Phys.* **4** 1438 (2002)
17. V A Radzig, L Yu Ustinuik, N Yu Osokina, V I Pergushev, M Yu Mel'nikov *J. Phys. Chem. A* **102** 5220 (1998)

18. M Yu Mel'nikov, V I Pergushov, N Ya Osokina *Spectrochim. Acta, Part A* **56** 2517 (2000)
19. K J Klabunde, C Gadenas-Trivino, in *Active Metals Preparation, Characterisation, Applications* (Ed. A Furster) (Weinheim: VCH, 1996) p. 237
20. E Ya Misochko, V A Benderskii, A U Goldschleger, A V Akimov *Mendeleev Commun.* 203 (1994)
21. V I Feldman, F F Sukhov, A Ya Orlov, N A Shmakova *J. Phys. Chem. A* **104** 37 921 (2000)
22. R Wagner, F Schouren, M S Gudipati *J. Phys. Chem. A* **104** 3593 (2000)
23. A L Buchachenko, E L Frankevich *Chemical Generation and Reception of Radio- and Microwaves* (New York: VCH, 1994)
24. N Z Lyakhov, V V Boldyrev *Izv. Sib. Otd. Akad. Nauk, Ser. Khim. Nauk* **12** (5) 3 (1983)
25. I M Barkalov, D P Kiryuhin *Int. Rev. Phys. Chem.* **19** (1) 1 (2000)
26. E Ya Misochko, A V Akimov, I U Goldschleger, C A Wight *J. Chem. Phys.* **116** 10318 (2002)
27. A P Alivisatos *J. Phys. Chem.* **100** 13226 (1996)
28. E L Nagaev *Usp. Fiz. Nauk* **162** (9) 49 (1992) [a]
29. R A Andrievskii *Usp. Khim.* **63** 431 (1994) [*Russ. Chem. Rev.* **63** 411 (1994)]
30. A I Gusev *Usp. Fiz. Nauk* **168** (1) 55 (1998) [*Physics-Uspekhi* **41** 49 (1998)]
31. V I Roldugin *Usp. Khim.* **69** 899 (2000) [*Russ. Chem. Rev.* **69** 821 (1998)]
32. C N R Rao, G U Kularni, P Y Tomas, P P Edwards *Chem. Soc. Rev.* **29** 27 (2000)
33. I P Suzdalev, P I Suzdalev *Usp. Khim.* **70** 203 (2001) [*Russ. Chem. Rev.* **70** 177 (2001)]
34. A Alonso *Chem. Rev.* **100** 637 (2000)
35. M Vogel, K Hansen, A Herlet, L Schweikhard, C Walter *J. Chem. Phys.* **116** 9658 (2002)
36. N A Solov'ev, A V Solov'ev, W Greiner *Phys. Rev. A* **65** 053 203 (2002)
37. U Kreibig, M Volmer *Optical Properties of Metal Clusters* (Berlin, Heidelberg: Springer, 1995)
38. A Henglein *J. Phys. Chem. B* **104** 1206 (2000)
39. B G Ershov *Izv. Akad. Nauk, Ser. Khim.* 1733 (2000) [b]
40. G B Sergeev *Zh. Ros. Khim. O-va im. D I Mendeleeva* **46** (5) 22 (2002) [c]
41. G B Sergeev, M Yu Efremov *Mol. Cryst. Liq. Cryst.* **278** 17 (1996)
42. M Yu Efremov, A F Batsulin, G B Sergeev *Mendeleev Commun.* 7 (1999)
43. M A El-Sayed *J. Phys. Chem.* **95** 3898 (1991)
44. V V Barelko, I M Barkalov, V I Gol'danskii, A M Zanin, D P Kiryukhin *Avtovolnovye Rezhimy Prevrashcheniya v Nizko-temperaturnoi Khimii Tverdogo Tela. Preprint IKhF Akad. Nauk SSSR* (Autowave Regimes of Conversion in the Low-Temperature Solid State Chemistry. Preprint of Institute of Chemical Physics, Academy of Sciences of the USSR), Chernogolovka, 1988
45. I M Barkalov, D P Kiryukhin, S I Kuzina, P S Mozhaev, A I Mikhailov *Khim. Vys. Energ.* **30** 393 (1996) [d]
46. B Mile, Ph D Sillman, A R Yacob, J A Howard *J. Chem. Soc., Dalton Trans.* 653 (1996)
47. C Felix, C Sieber, W Harbick, J Buttet, I Rabin, W Schulze, G Ertl *Phys. Rev. Lett.* **86** 2992 (2001)
48. H Hoevel, B Grimm, M Pollmann, B Reihl *Eur. Phys. J. D* **9** 595 (1999)
49. S Fedrigo, W Harbich, J Buttet *J. Chem. Phys.* **99** 5712 (1993)
50. W E Klotzbuecher, M A Petrukhina, G B Sergeev *J. Phys. Chem. A* **101** 4548 (1997)
51. A V Nemukhin, A Yu Ermilov, M A Petrukhina, J Smetz, W E Klotzbuecher *Spectrochim. Acta, Part A* **53** 1803 (1997)
52. K R Asmis, M Brummer, C Kaposta, G Santambrogio, G von Helden, G Meijer, K Rademann, L Woeste *Phys. Chem. Chem. Phys.* **4** 1101 (2002)
53. H Hess, K R Asmis, T Leisner, L Woeste *Eur. Phys. J.* **16** 145 (2001)
54. G Wrigge, M Ausruc-Hoffmann, B V Issendorff *Phys. Rev. A* **65** 063201 (2002)
55. M Lorenz, V E Bondybey *J. Low Temp. Phys.* **26** 778 (2000)
56. A M Smith-Gicklhorn, M Frankowski, V E Bondybey *Phys. Chem. Chem. Phys.* **4** 1425 (2002)
57. J Mascetti, F Galan, I Papai *Coord. Chem. Rev.* **190** 557 (1999)
58. F G N Cloke *Chem. Soc. Rev.* 17 (1993)
59. L Andrews, A L Waida *Organometallics* **7** 743 (1988)
60. M L McKee *J. Am. Chem. Soc.* **115** 9608 (1993)
61. Y K Lee, L Manceron *J. Phys. Chem. A* **101** 9650 (1997)
62. V A Apkarian, N Schwentner *Chem. Rev.* **99** 1481 (1999)
63. V E Bondybey, M Lorenz *J. Low Temp. Phys.* **122** 509 (2001)
64. J Eloranta, K Vaskonen, H Hakkanen, T Kiljunen, H Kunntu *J. Chem. Phys.* **109** 7784 (1998)
65. E V Savchenko, O N Grigorashenko, A N Ogurtsov, V V Rudenkov, M Lorenz, M Frankowski, A M Smith-Gicklhorn, V E Bondybey *J. Lumin.* **94** 475 (2001)
66. E V Savchenko, O N Grigorashenko, A N Ogurtsov, V V Rudenkov, G B Gumenchuk, M Lorenz, M Frankowski, A M Smith-Gicklhorn, V E Bondybey *Surf. Sci.* **507–510** 753 (2002)
67. V G Storchak, J H Brehwer, G D Morris *Phys. Rev. Lett.* **75** 2384 (1995)
68. V G Storchak, J H Brehwer, G D Morris *Phys. Rev. Lett.* **82** 2729 (1999)
69. M A Strzhemechnyi, A A Solodovnik, S I Kovalenko *Fiz. Nizk. Temp.* **24** 669 (1998)
70. F Galan, M Fouassier, M Tranquille, J Mascetti, I Papai *J. Phys. Chem. A* **101** 2626 (1997)
71. I Papai, J Mascetti, R Fournier *J. Phys. Chem. A* **101** 4465 (1997)
72. F Elustondo, J Mascetti, I Papai *J. Phys. Chem. A* **104** 3572 (2000)
73. I Papai, Y Hannachi, S Gwizdala, J Mascetti *J. Phys. Chem. A* **106** 4181 (2002)
74. L Papai, G Shubert, Y Hannachi, J Mascetti *J. Phys. Chem. A* **106** 9551 (2002)
75. G B Sergeev *Vestn. Mosk. Univ., Ser. 2, Khim.* **42** 300 (2001) [e]
76. G B Sergeev, O V Zagorskaya *Vestn. Mosk. Univ., Ser. 2, Khim.* **28** 362 (1987) [e]
77. V V Zagorsky, G B Sergeev *Mol. Cryst. Liq. Cryst.* **186** 81 (1990)
78. V N Soloviev, E V Polikarpov, A V Nemukhin, G B Sergeev *J. Phys. Chem. A* **103** 6721 (1999)
79. D-Y Hwang, A M Mebel *J. Phys. Chem. A* **104** 7646 (2000)
80. G B Sergeev, T I Shabatina, V N Soloviev, A V Nemukhin *Spectrochim. Acta, Part A* **56** 2527 (2000)
81. A S Tulegenov, V N Solov'ev, G B Sergeev *Nauchnaya Sessiya MIFI (Sbornik Nauchnykh Trudov)* **9** 203 (2002)
82. V N Soloviev, G B Sergeev, A V Nemukhin, S K Burt, I A Topol' *J. Phys. Chem. A* **101** 8625 (1997)
83. S P Mikhalev, V N Soloviev, G B Sergeev, in *Proceedings of the 4th ICLTC, Keuruu, 2002* p. 205
84. G B Sergeev, V V Zagorsky, F Z Badaev *J. Organomet. Chem.* **243** 123 (1983)
85. V V Smirnov, L A Tyurina *Usp. Khim.* **63** 57 (1994) [*Rus. Chem. Rev.* **63** 55 (1994)
86. K J Klabunde, A Whetten *J. Am. Chem. Soc.* **108** 6529 (1986)
87. G B Sergeev, V V Zagorskii, M V Grishechkina *Metallorg. Khim.* **1** 1187 (1988) [f]
88. G B Sergeev, V S Komarov, I G Tarkhanova *Kinet. Katal.* **31** 209 (1990) [g]
89. K J Klabunde, G H Jeong, A W Olsen, in *Selective Hydrocarbon Activation: Principles and Progress* (Eds J A Davies, P L Watson, A Greenberg, J F Liebman) (New York: VCH, 1990) p. 433
90. Z H Kafafi, R H Hauge, L Fredin, W E Billups, J L Margrave *J. Chem. Soc., Chem. Commun.* 1230 (1983)
91. Y Yamada, K Katsumata *Chem. Lett.* **7** 746 (2000)
92. Y Yamada, H Shimasaki, Y Okamura, Y Ono, K Katsumata *Appl. Radiat. Isot.* **54** 21 (2001)
93. Y Yamada, K Katsumata, H Shimasaki, Y Ono, K Yamaguchi *Bull. Chem. Soc. Jpn.* **75** 277 (2002)
94. P L Arnold, F G N Cloke, P B Hitchcock *Chem. Commun.* **5** 481 (1997)
95. P L Arnold, F G N Cloke, K Khan, P Scott *J. Organomet. Chem.* **528** 77 (1997)
96. T I Shabatina, A V Vlasov, E V Vovk, G B Sergeev *Spectrochim. Acta* **56** 2539 (2000)
97. A V Vlasov, T I Shabatina, G B Sergeev *Zh. Fiz. Khim.* **76** 1981 (2002) [h]

98. V A Tolkachev, in *Kinetic Description of the Simplest Bimolecular Reactions in Organic Solids, in Reactivity of Molecular Solids* (Eds E Boldyreva, V Boldyrev) (Chichester: Wiley, 1999) p. 175
99. M P Egorov, A A Basova, A M Gal'minas, O M Nefedov, A A Moiseeva, R D Rahimov, K P Butin *J. Organomet. Chem.* **574** 279 (1999)
100. C Elschenbroich, J Hurley, B Metz, W Massa, G Baum *Organometallics* **9** 889 (1990)
101. G N Glavee, B R Jagidar, J J Schneider, K J Klabunde, L J Radonovich, K Dodd *Organometallics* **11** 1043 (1992)
102. E Elustondo, M Dalibart, J Deroult, J Mascetti *Phys. Chem. Earth, Part C* **24** 583 (1999)
103. A Klotz, P Marty, P Boissel, G Serra, B Chaudret, J P Daudley *Astron. Astrophys.* **304** 520 (1995)
104. A Klotz, P Marty, G Serra, D de Carro, G Serra, J Mascetti, P Parseval, J P Derounault, B Chaudret *Planet Space Astrophys. Sci.* **44** 957 (1996)
105. P Marty, P Parseval, A Klotz, B Chaudret, G Serra, P Boissel *Chem. Phys. Lett.* **256** 669 (1996)
106. M Rall, D Zhou, E G Hisvarsanyi, N S Sullivan *Phys. Rev. B* **45** 2800 (1992)
107. E G Hisvarsanyi, N S Sullivan *Phys. Rev. B* **48** 16577 (1993)
108. T Momose, M Miki, T Wakabayashi, T Shida, M C Chau, S S Lee, T Oka *J. Chem. Phys.* **107** 7707 (1997)
109. T Momose, T Shida *Bull. Chem. Soc. Jpn.* **71** 1 (1998)
110. J P Toennies, A F Vilesov, K B Whaley *Phys. Today* **54** 31 (2001)
111. Y Kwon, P Huang, M V Patel, D Blume, K B Whaley *J. Chem. Phys.* **113** 6469 (2000)
112. A V Benderskii, I Floranta, P Zadoyan, V A Apkarian *J. Chem. Phys.* **117** 1201 (2002)
113. J Eloranta, N Schwentner, V A Apkarian *J. Chem. Phys.* **116** 4039 (2002)
114. T Wakabayashi, T Momose *J. Chem. Phys.* **111** 4191 (1999)
115. R J Hinde, D T Anderson, S Tam, M E Fajardo *Chem. Phys. Lett.* **356** 355 (2002)
116. R J Hidle, D T Anderson, S Tam, N E Fajardo *Chem. Phys. Lett.* **356** 355 (2002)
117. T R Geballe, T Oka *Nature (London)* **384** 334 (1996)
118. M Gordonnier, D Hy, R M Dickson, R E Kerr, Y Zhang, T Oka *J. Chem. Phys.* **113** 3181 (2000)
119. J A Northby *J. Chem. Phys.* **115** 10 065 (2001)
120. T Diederich, T Doppner, J Braune, J Tiggesbaumker, K-H Meiwes-Broer *Phys. Rev. Lett.* **86** 4807 (2001)
121. S Vongehr, A A Scheidemann, C Wittig, V V Kresin *Chem. Phys. Lett.* **353** 89 (2002)
122. F Federmann, K Hoffmann, N Quaas, J P Toennies *Eur. Phys. J. D* **9** 11 (1999)
123. T Doppner, T Diederich, J Tiggesbaumker, K H Meiwes-Broer *Eur. Phys. J. D* **16** 13 (2001)
124. C P Shulz, P Claas, F Stienkemeier *Phys. Rev. Lett.* **8715** 3401 (2001)
125. F R Brühl, R A Trasca, W E Ernst *J. Chem. Phys.* **115** 10 220 (2001)
126. D Ievlev, I Rabin, W Schulze, G Ertl *Chem. Phys. Lett.* **328** 142 (2000)
127. T Diederich, J Tiggesbaümker, K H Meiwes-Broer *J. Chem. Phys.* **116** 3263 (2002)
128. U Even, J Jortner, D Noy, C Cossart-Magos *J. Phys. Chem.* **112** 8068 (2000)
129. A Heidenreich, U Even, J Jortner *J. Phys. Chem.* **115** 10 175 (2001)
130. A A Vostrikov *Zh. Inzh. Termofiz.* **3** (2) 99 (1993)
131. L P Mezhov-Deglin, A M Kokotin *Fiz. Nizk. Temp.* **28** 235 (2002)
132. L P Mezhov-Deglin, A M Kokotin *J. Low Temp. Phys.* **126** 697 (2002)
133. S I Kiselev, V V Khmelenko, D M Lee, V Kiryuhin, R E Boltnev, E B Gordon, B Keimer *Phys. Rev. B* **65** 024517 (2002)
134. S I Kiselev, V V Khmelenko, D M Lee, C Y Lee *J. Low Temp. Phys.* **128** 37 (2002)
135. T Kumada, S Mori, J Kumagai, Y Aratono, T Miyazaki *J. Phys. Chem. A* **103** 8966 (1999)
136. T Miyazaki, S Mori, T Nagasaka, Y Aratono, J Kumagai, T Kumada *J. Phys. Chem. A* **104** 9403 (2000)
137. T Kumada, M Sakakibara, T Nagasaka, H Fukuta, I Kumagai, T Miyazaki *J. Chem. Phys.* **116** 1109 (2002)
138. T Takayanagi, A Wada *Chem. Phys.* **277** 313 (2002)
139. K Komaguchi, T Kumada, T Takayanagi, Y Aratono, M Shiotani, T Miyasaki *Chem. Phys. Lett.* **300** 257 (1999)
140. M Fushitani, T Shida, T Momose, M Rasanen *J. Phys. Chem. A* **104** 3635 (2000)
141. M Fushitani, T Momose *J. Chem. Phys.* **116** 10 739 (2002)
142. K Hiraoka, T Takayma, A Euchi, H Haunda, T Sato *Astrophys. J.* **532** 1039 (2000)
143. K Hiraoka, T Sato, S Sato, T Takayama, N Sogoshi, S Katagawa *J. Phys. Chem. B* **106** 4974 (2002)
144. K Hiraoka, T Sato *Radiat. Phys. Chem.* **60** 389 (2001)
145. V I Gol'danskii, L I Trakhtenberg, V N Flerov *Tunnel'nye Yavleniya v Khimicheskoi Fizike* (Tunnel Effects in Chemical Physics) (Moscow: Nauka, 1986)
146. V I Goldanskii, V A Benderskii, L I Trakhtenberg *Adv. Chem. Phys.* **75** 349 (1989)
147. L I Trakhtenberg, V Sh Flombenlit *Zh. Fiz. Khim.* **67** 1631 (1993) [h]
148. V A Benderskii, D A Makarov, C A Wight *Chemical Dynamics at Low Temperatures* (New York: Wiley, 1994)
149. G K Ivanov, M A Kozhushner, L I Trakhtenberg *J. Chem. Phys.* **113** 1992 (2000)
150. G B Sergeev *Mol. Cryst. Liq. Cryst.* **313** 155 (1998)
151. G B Sergeev, V V Smirnov, M I Shilina, T N Rostovshikova *Mol. Cryst. Liq. Cryst.* **161** 201 (1988)
152. M Yu Efremov, V S Komarov, G B Sergeev *Mol. Cryst. Liq. Cryst.* **248** 111 (1994)
153. V A Kabanov, V G Sergeev, G M Lukovkin, V Yu Baranovskii *Dokl. Akad. Nauk SSSR* **266** 1410 (1982) [i]
154. V I Goldanskii *Nature (London)* **279** 109 (1979)
155. M Bernstein, S A Sandford, L J Allamandola, J S Gillette, S J Clemett *Science* **283** 1135 (1999)
156. V V Barelko, I M Barkalov, V I Goldanskii, D P Kiryuhin, A M Zanin *Adv. Chem. Phys.* **74** 339 (1988)
157. D P Kiryukhin, P S Mozhaev, V V Barelko, I M Barkalov *Khim. Fiz.* **11** 264 (1992) [j]
158. P S Mozhaev, G A Kichigina, D P Kiryuhin, I M Barkalov *Mendeleev Commun.* 64 (1993)
159. S P Gubin *Zh. Ros. Khim. O-va im. D I Mendeleeva* **46** (5) 32 (2002) [c]
160. Yu I Petrov *Klastery i Malye Chastitsy* (Clusters and Small Particles) (Moscow: Nauka, 1986)
161. A I Gusev *Nanokristallicheskie Materialy: Metody Polucheniya i Svoistva* (Nanocrystalline Materials: Preparation Methods and Properties) (Ekaterinburg: Institute of Solid State Chemistry, Urals Branch of the Russian Academy of Sciences, 1998)
162. A D Pomogailo, A S Rozenberg, I E Uflyand *Nanochastitsy Metallov v Polimerakh* (Nanoparticles of Metals in Polymers) (Moscow: Khimiya, 2000)
163. K Kimura, S Bandow *Bull. Chem. Soc. Jpn.* **56** 3578 (1983)
164. K Bromann, C Felix, H Brune, W Harbich, R Monot, J Buttet, K Kern *Science* **274** 956 (1996)
165. S J Carroll, S Pratontep, M Streun, R E Palmer, S Hobday, R Smith *J. Chem. Phys.* **113** 7723 (2000)
166. H-V Roy, P Fayet, F Pathey, W-D Schneider, B Delley, C Massobrio *Phys. Rev. B* **49** 5611 (1994)
167. B M Sergeev, G B Sergeev, Y J Lee, A N Prusov, V A Polyakov *Mendeleev Commun.* 151 (1997)
168. B M Sergeev, G B Sergeev, A N Prusov *Mendeleev Commun.* 1 (1998)
169. B M Sergeev, G B Sergeev, V A Kasaikin, E A Litmanovich, A N Prusov *Mol. Cryst. Liq. Cryst.* **356** 121 (2001)
170. F Z Badaev, V A Batyuk, A M Golubev *Vestn. Mosk. Univ., Ser. 2, Khim.* **36** 390 (1995) [c]
171. G N Glavee, K Easom, K J Klabunde, C M Sorensen, G C Hadjipanayis *Chem. Mater.* **4** 1360 (1992)
172. K J Klabunde, D Zhang, G N Glavee, C M Sorensen *Chem. Mater.* **6** 784 (1994)
173. N Sun, K J Klabunde *J. Catal.* **185** 506 (1999)

174. G N Clavee, C F Kernizan, K J Klabunde, C M Sorensen, G C Hadjipanayis *Chem. Mater.* **3** 967 (1991)
175. F Henglein, A Henglein, P Mulvaney *Ber. Bunsen-Ges. Phys. Chem.* **98** 180 (1994)
176. V I Bukhtiyarov, M G Slin'ko *Usp. Khim.* **70** 167 (2001) [*Russ. Chem. Rev.* **70** 147 (2001)]
177. T N Boronina, I Lagadic, G B Sergeev, K J Klabunde *Environ. Sci. Technol.* **32** 2614 (1998)
178. K J Klabunde (Ed.) *Nanoscale Materials in Chemistry* (New York: Wiley, 2001)
179. A S Edelstein, R C Cammarata (Eds), in *Nanomaterials: Synthesis, Properties and Applications* (Bristol, Philadelphia: Inst. of Physics Publ., 1998) p. 596
180. Z L Wang (Ed.) *Characterisation of Nanophase Materials* (Weinheim, New York, Chicherster, Singapore, Toronto: Wiley-VCH-Verlag Chemie-GmbH, 2000)
181. Y Finkelstein, R Moreh, O Shahal *Surf. Sci.* **437** 265 (1999)
182. R B Shirazi, K Knorr *Surf. Sci.* **243** 303 (1991)
183. K Madih-Ayadi, S Rakotozafy, T Ceva, B Croset, N Dupont-Pavlovsky, P Convert, I Mirebeau, E Ressouche *Surf. Sci.* **436** 99 (1999)
184. D Fuhrmann, R Gerlach, H G Rubahn, Ch Woll *Surf. Sci.* **424** 145 (1999)
185. M A Reed, C Zhou C J Muller, T P Burgin, J M Tour *Science* **278** 252 (1997)
186. P H Dhirani, P Lin, R W Guyot-Sionnest, L R Zehner, L R Sita *J. Chem. Phys.* **106** 5249 (1997)
187. V K Gupta, J J Skaife, T B Dubrovsky, N L Abbout *Science* **279** 2077 (1998)
188. X Y Zhu, T Vondrak, H Wang, C Gahl, K Ishioka, M Wolf *Surf. Sci.* **451** 244 (2000)
189. K Oura, T Hanawa *Surf. Sci.* **82** 202 (1979)
190. F Komori, K Kushida, K Hottori, S Arai, T Limori *Surf. Sci.* **438** 123 (1999)
191. F Moresco, M Rocco, T Hildebrant, M Henzler *Surf. Sci.* **463** 22 (2000)
192. T Bornemann, A Otto, W Heuer, H Zacharias *Surf. Sci.* **420** 224 (1999)
193. K A Edwards, P B Howes, J E Macdonald, T Hibma, T Bootsma, M A James *Surf. Sci.* **424** 169 (1999)
194. F Bocquet, S Robert, S Gauthier, J L Duvault, J Klein *Surf. Sci.* **392** 86 (1997)
195. H Petek, M J Weida, H Nagano, S Ogawa *Surf. Sci.* **451** 22 (2000)
196. L Abelmann, S Porthun, M Haast, C Lodder, A Moser, M E Best, P J A van Schendel, B Steifel, H J Hug, G P Heydon, A Farley, S R Hoon, T Pfaffelhuber, R Proksch, K Babcock *J. Magn. Magn. Mater.* **190** 135 (1998)
197. D Purdie, M Hengsberger, M Garnier, Y Baer *Surf. Sci.* **407** L671 (1999)
198. Heinrich, M Kowalewski, J F Cochran *Can. J. Chem.* **76** 1595 (1998)
199. E Heifets, Y F Zhukovskii, E A Kotomin, M Causa *Chem. Phys. Lett.* **283** 395 (1998)
200. M H Schaffner, F Patthey, W D Schneider *Surf. Sci.* **417** 159 (1998)
201. T Kodas, M Hampden-Smith (Eds) *The Chemistry of Metal CVD* (Weinheim, New York, Basel, Cambridge, Tokyo: VCH, 1994)
202. S Sato, Y Ukisu, H Ogawa, Y Takasu *J. Chem. Soc., Faraday Trans.* **89** 4387 (1993)
203. L Sun, E M McCash *Surf. Sci.* **422** 77 (1999)
204. Johnson, E T Jensen *Surf. Sci.* **451** 261 (2000)
205. W Zhao, C Kim, J M White *Surf. Sci.* **451** 267 (2000)
206. Y M Sun, D Sloan, H Ihm, J M White *J. Vac. Sci. Technol., A* **14** 1516 (1996)
207. C Bater, M Sanders, J H Craig Jr *Surf. Sci.* **451** 226 (2000)
208. V Andryushechkin, K N Eltsov, V M Shelyuga, C Tarducci, B Cortigiani, U Bardi, A Atrei *Surf. Sci.* **421** 27 (1999)
209. R J M Vullers, M Ahlskog, C van Haesendock *Appl. Surf. Sci.* **144–145** 584 (1999)
210. M Tabe, T Yamamoto, Y Terao *Appl. Surf. Sci.* **117** 131 (1997)
211. S K Jo, B Gong, G Hess, J M White, J G Ekerdt *Surf. Sci.* **394** L162 (1997)
212. G Wu, D Staechiola, M Kalchev, W T Tysoe *Surf. Sci.* **463** 81 (2000)
213. S Bougreois, R Gouttebraon, M Perderaeu *Surf. Sci.* **395** 356 (1998)
214. G S Jones, M A Barteau, J M Vohs *Surf. Sci.* **420** 65 (1999)
215. S L Silva, R M Lemor, F M Leibsle *Surf. Sci.* **421** 146 (1999)
216. B E Salisbury, W T Wallace, R L Whetten *Chem. Phys. Lett.* **262** 131 (2000)
217. W T Wallace, R L Whetten *J. Phys. Chem. B* **104** 10964 (2000)
218. W T Wallace, R L Whetten *J. Am. Chem. Soc.* **124** 7499 (2002)
219. A Dinger, C Lutterloh, J Biener, J Kuppers *Surf. Sci.* **437** 116 (1999)
220. M A Petrukhina, L N Aleksandrova, V V Zagorskii, G B Sergeev, I E Kardash, G N Gerasimov, in *Materialy Konferentsii po Khimii Nizkikh Temperatur* (Proceedings of the Conference on Low-Temperature Chemistry) (Moscow: Moscow State University, 1991) p. 130
221. L N Aleksandrova, L V Shundina, G N Gerasimov, I E Kardash *Vysokomol. Soedin., Ser. A* **35** 361 (1993) [j]
222. G B Sergeev, V V Zagorsky, M A Petrukhina *J. Mater. Chem.* **5** 31 (1995)
223. Russ. P. 2 017 547; *Ref. Zh. Khim.* 4 L 101P (1995)
224. G B Sergeev, M A Petrukhina *Prog. Solid State Chem.* **24** 183 (1996)
225. V V Zagorskii, V E Botchenkov, S V Ivashko, G B Sergeev *Nanostruct. Mater.* **12** 863 (1999)
226. G B Sergeev, V V Zagorsky, M A Petrukhina, S A Zav'yalov, E I Grigor'ev, L I Trakhtenberg *Anal. Commun.* **34** 113 (1997)
227. L Alexandrova, E Sansores, E Martinez, E E Rodriquez, G Gerasimov *Polymer* **42** 273 (2001)
228. P S Vorontsov, E I Grigor'ev, S A Zav'yalov *Khim. Fiz.* 21 (2001) [j]
229. L I Trakhtenberg, G N Gerasimov, V K Potapov, T N Rostovshchikova, V V Smirnov, V Yu Zufman *Vestn. Mosk. Univ., Ser. 2, Khim.* **42** 325 (2001) [e]
230. V E Bochenkov, N Stephan, L Brehmer, V V Zagorskii, G B Sergeev *Colloids Surf. A* **198** 911 (2002)
231. T I Shabatina, E V Vovk, N V Ozhegova, A V Nemukhin, G B Sergeev *Mater. Sci. Eng. C* **8–9** 53 (1999)
232. T I Shabatina, E V Vovk, V A Timoshenko, Yu N Morozov, G B Sergeev *Vestn. Mosk. Univ., Ser. 2, Khim.* **42** 314 (2001) [e]
233. T I Shabatina, E V Vovk, V A Timoshenko, Yu N Morosov, G B Sergeev *Colloids Surf. A* **198** 255 (2002)
234. N V Ozhegova, A V Nemukhin, T I Shabatina, G B Sergeev *Mendeleev Commun.* 218 (1998)
235. V T Aleksanyan, B V Lokshin *Kolebatel'nye Spektry π-Kompleksov Perekhodnykh Elementov. Stroenie Molekul i Khimicheskaya Svyaz' (Itogi Nauki i Tekhniki)* [Vibrational Spectra of π-Complexes of Transition Elements. Structure of Molecules and Chemical Bond. (Advances in Sciences and Engineering Series)] (Moscow: Izd. VINITI, 1976)
236. R A Zeinalov, L M Blinov, M F Grebenkin, B I Ostrovskii, M A Saidakhmetov *Kristallografiya* **33** 185 (1998) [l]
237. T I Shabatina, V A Timoshenko, Yu N Morosov, G B Sergeev *Mater. Sci. Eng.* **22** 193 (2002)
238. E V Polikarpov, T I Shabatina, G B Sergeev, A V Nemukhin *Vestn. Mosk. Univ., Ser. 2, Khim.* **41** 283 (2000) [e]
239. T I Shabatina *Zhid. Kristal. Prakt. Ispol.* **1** 58 (2002) [m]
240. L M Bronstein, D M Chernyshov, P M Valetsky, E A Wilder, R J Spontak *Langmuir* **16** 8221 (2000)
241. M Hyslop, A Wurl, S A Brocon, D D Hall, R Monot *Eur. Phys. J. D* **16** 233 (2001)
242. X M Lin, C M Sorensen, K J Klabunde *Chem. Mater.* **11** 198 (1999)
243. F Tian, K J Klabunde *New J. Chem.* 1275 (1998)
244. S Fullam, S N Rao, D Fitzmaurice *J. Phys. Chem. B* **104** 6164 (2000)
245. A Kumar, A B Mandale, M Sastry *Langmuir* **16** 6921 (2000)
246. A K Boal, F Ilhan, J E De Rouchey, Th Thurn-Albrecht, Th P Russell, V M Rotello *Nature (London)* **404** 746 (2000)
247. B Nikoobakht, Z L Wang, M A El-Sayed *J. Phys. Chem. B* **104** 8635 (2000)
248. B Kaiser, B Stegemann, H Kaukel, K Rademann *Surf. Sci.* **496** 218 (2002)

249. T P Darby, C M Wayman *J. Cryst. Growth* **29** 98 (1985)
250. R Anton, I Scheidereit *Phys. Rev. B* **58** 13874 (1998)
251. L Motte, E Lacaze, M Maillard, M P Pileni *Langmuir* **16** 3803 (2000)
252. J F Kang, J Zaccaro, A Ulman, A Myerson *Langmuir* **16** 3791 (2000)
253. H Fukushima, S Seki, T Nishikawa, H Takiguchi, K Tamada, K Abe, R Colorado Jr, M Graupe, O E Shmakova, T R Lee *J. Phys. Chem. B* **104** 7417 (2000)
254. T Yonezawa, S Onone, N Kimizuka *Adv. Mater.* **13** 140 (2001)
255. T Yonezawa, K Yasui, N Kimizuka *Langmuir* **17** 271 (2001)
256. L Maya, E A Kenik *Langmuir* **16** 9151 (2000)
257. Ch A Mirkin, T A Taton *Nature (London)* **405** 626 (2000)
258. S R Whaley, D S English, E L Hu, P F Barbara, A M Belcher *Nature (London)* **405** 665 (2000)
259. P M Tessier, O D Velev, A T Kalambur, J F Rabolt, A M Lenhoff, E W Kaler *J. Am. Chem. Soc.* **122** 9554 (2000)
260. R E Palmer *Nature (London)* **408** 531 (2000)
261. J J Storhoff, A A Lazarides, R C Mucic, C A Mirkin, R L Letsinger, G C Schatz *J. Am. Chem. Soc.* **122** 4640 (2000)
262. G B Sergeev, T I Shabatina, in *Frontiers in Surface and Interface Science* (Eds Ch B Duke, E W Plummer) (New York: Elsevier, 2002) p. 628
263. G B Sergeev *Nanokhimiya* (Nanochemistry) (Moscow: Moscow State University, 2003)
264. M C Roco, R S Williams, P Alivisatos (Eds) *Nanotechnology Research Directions: IWGN Workshop Report. Vision for Nanotechnology in the Next Decade* (Dordrecht: Kluver Academic, 2000)
265. A L Buchachenko *Usp. Khim.* **72** 419 (2003) [*Russ. Chem. Rev.* **72** 375 (2003)]

[a] — *Physics-Uspekhi (Engl. Transl.)*
[b] — *Russ. Chem. Bull., Int. Ed. (Engl. Transl.)*
[c] — *Mendeleev Chem. J. (Engl. Transl.)*
[d] — *High Energy Chem. (Engl. Transl.)*
[e] — *Moscow Univ. Bull. (Engl. Transl.)*
[f] — *Organomet. Chem. (Engl. Transl.)*
[g] — *Kinet. Catal. (Engl. Transl.)*
[h] — *Russ. J. Phys. Chem. (Engl. Transl.)*
[i] — *Dokl. Chem. (Engl. Transl.)*
[j] — *Chem. Phys. Rep. (Engl. Transl.)*
[k] — *Polym. Sci. (Engl. Transl.)*
[l] — *Crystallogr. Rep. (Engl. Transl.)*
[m] — *Liquid Cryst. Appl. (Engl. Transl.)*